1   Glycolysis plays an important role in energy transfer from the base to the distal end of the flagellum in

2   mouse sperm.

3

4   Gen L. Takei*, Daisuke Miyashiro, Chinatsu Mukai** and Makoto Okuno***

5   Department of Life Sciences, Graduate School of Arts and Sciences, The University of Tokyo Komaba

6   3-8-1, Meguro-ku, Tokyo, 153-8902 Japan

7

8   Present affiliations

9   *Cardiovascular Physiology, Okayama University Graduate School of Medicine, Dentistry and

10   Pharmaceutical Science 2-5-1, Shikada-cho, Kita-ku, Okayama-city, Okayama 700-8558 Japan

11 **Baker Institute for Animal Health, College of Veterinary Medicine, Cornell University, Ithaca, NY

12   14853, USA

13 ***Department of Biology, Chuo University 1-13-27 Kasuga, Bunkyo-ku, Tokyo 112-8551 Japan

14 ***Send correspondence to

15

16

17

18 Running title: Glycolysis in mouse sperm flagella

19 Key words: mammalian sperm, motility, glycolysis, energy transport, metabolism, flagellar bending

20

21

22

23

Summary

25   Since many of studies have been conducted to elucidate the relationship between energy

26   metabolic pathways (glycolysis and respiration) and flagellar motility in mammalian sperm,

27   contribution of glycolysis to sperm motility has not been fully elucidated yet. In the present study,

28   we performed detailed analysis of mouse sperm flagellar motility for further understanding of the

29   contribution of glycolysis to mammalian sperm motility. Mouse sperm maintained vigorous

30   motility by substrates either for glycolysis or for respiration. By contrast, inhibition of glycolysis by

31   alpha-chlorohydrine (ACH) caused significant decrease in bend angle of flagellar bending wave,

32   sliding velocity of outer doublet microtubules and ATP content even in the presence of respiratory

33   substrates (pyruvate or beta-hydroxybutyrate; BHB). The decrease of flagellar bend angle and

34   sliding velocity are prominent in the distal part of the flagellum, indicating that glycolysis

35   inhibition caused the decrease in ATP concentration threrein. These results suggest that glycolysis

36   potentially act as a spatial ATP buffering system, transferring energy (ATP) synthesized by

37   respiration at mitochondria located in the basal part of the flagellum to the distal part. In order to

38   validate glycolytic enzymes can transfer high energy phosphoryls, we calculated intraflagellar

39   concentration profiles of adenine nucleotides along the flagellum by computer simulation analysis.

40   The result demonstrated the involvement of glycolysis for maintaining the ATP concentration at the

41   tip of the flagellum. It is likely that glycolysis plays a key role in energy homeostasis in mouse

42   sperm not only through ATP production but also through energy transfer.

43

Introduction

Mammalian sperm flagella require motility for a long period of time from ejaculation to accomplish fertilization (Austin, 1985). For the maintenance of motility during such a long period, mammalian sperm must continue to metabolize extracellular energy substrates for producing ATP. Therefore, elucidation of the correlation between flagellar movement and energy metabolism is very important to understand the functional feature of the mammalian sperm. Furthermore, it has been expected to be applied to the treatment of male infertility and contraceptive technologies.

There are two major metabolic pathways to produce ATP, glycolysis and respiration. Most mammalian sperm must produce ATP to keep vigorous motility by both or one of them, which are localized at different region of sperm. Mitochondria which perform respiration are localized in the mid-piece, the basal limited locus of flagellum. On the other hand, glycolysis works in the principal piece of flagella occupying major part of flagellum, since several glycolytic enzymes have been reported to be localized on the fibrous sheath, a cytoskeletal structure which goes through entire length of the sperm tail (Krisfalusi et al., 2006; Westhoff and Kamp, 1997). Because of higher efficiency of ATP production and an abundance of mitochondria in mammalian sperm, respiration has been considered to be a major source of ATP production.

Recent studies, however, demonstrated that glycolysis plays a major role for ATP production in mouse sperm flagellar movement (Mukai and Okuno, 2004). Glyceraldehyde-3-phosphate dehydrogenase (GAPDH), one of glycolytic enzyme that catalyzes glycelaldehyde-3-phosphate (GAP) to 1, 3-bisphosphoglycerate (1, 3BPG), is

66   abundantly localized to the fibrous sheath in porcine, human, bovine, equine and murine sperm

67   (Westhoff and Kamp, 1997; Welch et al., 2000). Genetic deletion of sperm specific isoenzyme

68   of GAPDH, GAPDS, using knock-out model gave rise to sperm immotility even in the

69   presence of pyruvate, a respiration substrates, resulting in infertility (Miki et al., 2004). In

70   addition to GAPDS, proteomic studies revealed that multiple glycolytic enzymes (hexokinase,

71   aldolase, phosphoglycerate kinase, enolase, pyruvate kinase and lactate dehydrogenase) were

72   demonstrated to localize in the fibrous sheath in mouse sperm (Krisfalusi et al., 2006). It was

73   also reported that the knock-out mouse of sperm specific glycolytic enzymes, lactate

74   dehydrogenase C (LDHC) and phosphoglycerate kinase 2 (PGK2), resulted in infertility in

75   mouse (Odet et al., 2008; Danshina et al., 2010). These studies supported that glycolysis in the

76   principal piece is a crucial ATP production pathway in mouse sperm.

77   Another serious problem that must be solved is how ATP synthesized in mitochondria at

78   the base of the flagellum is supplied sufficiently to the distal end of the flagellum, because ATP

79   is necessary at the end of the flagellum for the active bending movement. In sea urchin, the

80   problem is solved by "creatine shuttle", an energy transporting system from mitochondria at

81   the base to the tip of the flagella (Tombes et al., 1987). On the other hand, such an energy

82   transferring system has not been detected although mouse sperm has a longer flagellum (120

83   μm) than sea urchin sperm (40 μm) (Kamp et al., 1996). These results suggest that

84   mitochondria-synthesized ATP is not assumed to be supplied to the tip of flagellum sufficiently.

85   Based on these studies, it has been considered that ATP necessary for flagellar movement is

86   produced mainly by glycolysis.

87   On the other hand, there are some contradicting reports (Ford, 2006; Tanaka et al., 2004).

88   Tanaka and colleagues (2004) reported that a testis-specific isoenzyme of succinyl CoA

89   transferase (SCOT-t) is expressed in mouse sperm. SCOT-t is necessary to metabolize

90   D-β-hydroxybutyrate (BHB), a substrate of respiration. When BHB was supplemented to the

91   sperm suspension instead of glucose, the percentage of sperm motility was not affected by

92   α-chlorohydrin (ACH), a potent inhibitor of GAPDH. Moreover, it was reported that

93   intracellular ATP concentration was not decreased by ACH in the absence of glucose (Ford and

94   Harrison, 1985; Ford and Harrison, 1986). These results support that respiration is enough to

95   supply ATP for sperm motility.

96   As mentioned above, there are some contradictory results about the relationship between

97   metabolic pathways and sperm motility. These studies were focused on which metabolic

98   pathway (glycolysis or respiration) was important and dominant for sperm motility, and did

99   not address to the possibilities that these two metabolic pathways may contribute to the

100   flagellar movement differently. To investigate the possibility, more detailed analysis of

101   flagellar movement seems to be necessary.

102   In the previous studies, flagellar movement was assessed by the percentage of motile

103   sperm or the beat frequency of flagellum. However, these parameters were insufficient to

104   evaluate the "magnitude" of microtubule sliding, an important parameter for evaluating the

105   amount of microtubule sliding. Flagellar bending motion is produced through sliding of the

106   pairs of doublet microtubules by forces produced by dynein arms that hydrolyze ATP.

107   Therefore, microtubule sliding velocity, resulting from the rate of ATP hydrolysis, is directly

108   related to the ATP concentration which is the result of consumption and production. In order to

109   assess the contribution of ATP production pathways to the flagellar movement, sliding velocity

110 was calculated as a product of beat frequency and bend angle. It was reported that sliding

111 velocity correlates with ATP concentration (Yano and Miki, 1980; Si and Okuno, 1995).

112 Therefore, change of sliding velocity could be assumed to reflect the change of ATP

113 concentrations directly. Furthermore, the local bending along the flagellum is tightly coupled

114 to the local sliding velocity since the beat frequency of flagellum is constant throughout the

115 entire length of flagellum (Okuno and Hiramoto, 1976), and thus leads to an evaluation of

116 local concentrations of ATP therein.

117   In the present study, correlation between metabolic pathways, especially glycolysis, and

118 flagellar movement was re-evaluated by detailed motility analysis (measurement of beat

119 frequency, bend angle, sliding velocity and local bending). Finally, we found that glycolysis

120 was suggested to function as not only ATP production system, but also energy transferring

121 system through spatial buffering of ATP.

122

123

124

125

126

127

128

129

130

131

Results

132

Change of motility depending on metabolic substrates

133

First, differences of motility induced by substrates (Glucose, Pyruvate and BHB) were

134

evaluated by detailed analysis of flagellar movement using various parameters (beat frequency,

135

bend angle and sliding velocity of microtubules). Results are summarized in Table 1. Mouse

136

sperm commonly exhibited high motility (10< Hz beat frequency, 30< rad/sec sliding velocity)

137

at 10 mmol l^{-1} of each substrate, and very little difference of motility parameters (beat

138

frequency, bend angle, percentage of motility, sliding velocity and waveform of flagella) were

139

observed among them.

140

Effect of glycolysis inhibition on flagellar movement

141

Sperm maintained vigorous motility for more than 60 min either in the presence of

142

Glucose, pyruvate or BHB (Table 1). This result indicates that mouse sperm can produce

143

sufficient ATP to sustain motility by either glycolysis or respiration alone. Then, we observed

144

the effect of glycolysis inhibition on sperm motility to clarify the contribution of glycolysis on

145

sperm motility. Fig. 1 shows change of beat frequency, bend angle and sliding velocity with

146

time in the presence or absence of α-chlorohydrin (ACH). When glycolysis was inhibited by

147

ACH in the presence of glucose, mouse sperm stopped swimming by 60 minutes (Fig. 1). On

148

the other hand, beat frequency of sperm was not affected by ACH at least for 60 min, when

149

substrate for respiration, BHB or pyruvate, was added to the test solution (Fig. 1A) instead of

150

glucose. However, the bend angle of flagella was significantly inhibited by ACH at 30 and 60

151

minutes after activation even in the presence of BHB or pyruvate (Fig. 1B). As a result, sliding

152

velocity was significantly reduced by ACH to less than 30 rad/sec at 30 and 60 minutes after

153

154 activation (Fig. 1C). Similar results were obtained when glycolysis was inhibited by

155 2-deoxyglucose (DOG), an analog of glucose that inhibits hexokinase (Hiipakka and

156 Hammerstedt, 1978; Hyne and Edwards, 1985: Data not shown). Because sliding velocity was

157 known to correlate with ATP concentration (Yano and Miki, 1980; Si and Okuno, 1995), these

158 results indicated a decrease in intracellular ATP by ACH even in the presence of respiratory

159 substrates.

160 ***Effect of glycolysis inhibition on local bending of flagellum***

161 Glycolysis-inhibited sperm showed unchanged beat frequency and significantly reduced

162 bend angle in the presence of respiratory substrates. To further characterize the decrease of

163 bend angle, local bending along the flagellum was investigated in every 10 µm by measuring

164 the shear angle.

165 In the presence of respiratory substrates and absence of ACH, local shear angle in the

166 flagellum increased as the bending wave propagated to the distal end, except for a "singular

167 point" at 70 µm, where tangent line and reference line synchronously keep rather parallel

168 (BHB or pyruvate; Fig. 2A, B). On the other hand, sperm whose glycolysis was inhibited by

169 ACH did not show such an increase along the flagellar axis in the shear angle. The shear angle

170 of flagellum was almost unchanged from the basal region to the distal end of flagellum (Fig.

171 2A, B). Similar results were obtained with DOG. These results indicate that inhibition of

172 glycolysis abolished the increase in the shear angle toward the distal end of flagellum.

173 Data shown in Figure 2A, B were re-plotted as the ratio of local bending by dividing

174 shear angle in glycolysis-inhibited sperm by that in the control sperm (Fig. 2C, D). The ratio of

175 local bending of glycolysis-inhibited sperm was high at the basal region of flagellum (about

176   0.7), suggesting that the inhibition was low, but was considerably reduced at the tip of

177   flagellum (about 0.5).

178   In addition to the evaluation of local bending by the shear angle, local bending was

179   evaluated by the bend angle in order to eliminate the "singular point" observed in Fig. 2A and

180   B (Fig. 3). Similar to the result of shear angle (Fig. 2A, B), sperm showed gradual increase in

181   bending as wave propagated when glycolysis was not inhibited by ACH (filled symbols). By

182   contrast, glycolysis-inhibited sperm (open symbols) did not show so large increase as those

183   without ACH, consistent with the results of the shear angles (Fig. 2A and B). These results

184   indicate that reduction of bending is prominent in the distal region of flagellum.

185   ***Effect of glycolysis inhibition on the content of ANP in sperm***

186   Glycolysis-inhibited sperm showed decreased bend angles and sliding velocities despite

187   the presence of respiratory substrates, suggesting a decrease in ATP concentration. In order to

188   examine whether intracellular ATP was decreased or not, ANP content was directly measured

189   by reversed-phase high performance liquid chromatography (HPLC) in mouse sperm 30

190   minutes after activation. Fig. 4 shows the change in the ANP content by the inhibition of

191   glycolysis.

192   When glucose was added to the media as a metabolic substrate, a higher content of ATP

193   (about 0.4 nmol/10^6 sperm), and lower contents of ADP and AMP (approximately 0.16 and

194   0.07 nmol/10^6 sperm, respectively) were measured than in sperm incubated in the absence of

195   substrates. Similarly, high contents of ATP and low contents of ADP, AMP were observed in

196   the presence of respiratory substrates (Pyr and BHB). There was no significant difference

197   between them. ACH treatment, however, caused a drastic decrease in ATP ($p < 0.01$) content

and increase in AMP content (p<0.01) in the presence of glucose. ACH treatment also caused a

decrease in ATP content and increase in ADP and AMP in the presence of pyruvate and BHB.

These results suggest that inhibition of glycolysis by ACH causes metabolic perturbation even

in the presence of respiratory substrates.

Metabolome analysis

In order to determine the intracellular state of metabolic intermediates, metabolomic

analysis by CE-TOFMS was conducted (table 2). Intracellular ATP content determined by

metabolomic analysis was 0.368 nmol/10^6 sperm. This value was approximately the same as

that determined by HPLC (Fig. 4), indicating the accuracy of metabolomic analysis.

Calculated concentrations of total intracellular ANP and total PGK substrates (total 3PG and 1,

3BPG) were 11.6 mmol l^{-1} and 0.155 mmol l^{-1}, respectively (table 2). The values for the

cytosolic volume used to calculate the intracellular concentration of each parameter was 53.5

fL (Yeung et al., 2002). The values used for following computer simulation were shown in

Table 2.

Computer simulation

As described above, glycolysis inhibition caused the decrease in the sliding velocity at

the distal part of the flagellum, indicating the deficiency of ATP therein in spite of the presence

of respiratory substrates. These results suggest that ATP synthesized by mitochondria at the

base (mid piece) could not supply to the distal part of the flagellum sufficiently when

glycolysis is inhibited. This phenomenon raised the possibility that glycolysis functions as a

spatial buffering of ATP along mouse sperm flagellum, transferring "energy wave" from the

mid piece to the distal end.

220   In previous studies, it was reported that glycolytic enzymes, particularly

221   phosphoglycerate kinase (PGK), have a potential to transfer energy in muscle cells through

222   buffering of ATP (Dzeja et al., 2004; Dzeja and Terzic, 2003). To assess the possibility that

223   glycolysis has the potential to transport energy to the distal end of the flagellum in mouse

224   sperm, the concentrations of high energy phosphoryls (ATP and ADP) along the flagellum

225   were calculated by simulating the intraflagellar diffusion of high energy phosphoryls *in silico*.

226   The algorithms of the simulation were based on the simulation model by Tombes et al. that

227   verified energy transfer potential of creatine kinase in sea urchin sperm (Tombes et al., 1987).

228   The diffusing length of flagellum was set to 100 µm although murine sperm has a 120 µm

229   flagellum, because the mid piece, a mitochondria-rich region, is as long as 20 µm. Fig. 5.

230   illustrates the results of calculations of ATP, ADP and ATPase activity profile along the

231   flagellum.

232   It was reported that adenylate kinase (AK) also participates in energy transfer (Dzeja and

233   Terzic, 2003). Since AK is abundantly present throughout the mouse sperm flagella (Cao et al.,

234   2006), the reaction of AK was also considered in the equation. The parameters of AK used in

235   the simulation were obtained from the data on rabbit muscle AK (Noda, 1973). When the

236   reaction by AK is included and glycolysis (PGK) is excluded in the simulation, ATP at the tip

237   of the flagellum decreased from 11.4 mmol l^{-1} (basal concentration) to 5.45 mmol l^{-1}, whereas

238   ADP at the tip increased from 0.2 mmol l^{-1} (basal concentration) to 3.71 mmol l^{-1} (data not

239   shown). The ratio of the total amount of intraflagellar ATP to the total ADP calculated by

240   computer simulation was approximately 5:2 under this condition where only AK operates in

241   ATP transfer. This ratio was quite different from the ratio of the total intracellular ATP to total

242   intracellular ADP of glycolysis-inhibited sperm determined by HPLC analysis, which was

243   approximately 5:4 (Fig. 4). When both AK rate and PGK rate were reduced to zero, in other

244   words, when ATP at the distal region was assumed to be supplied only by simple diffusion

245   from the mid piece without ATP buffering, the ratio of the total intraflagellar ATP to the total

246   intraflagellar ADP was calculated to be approximately 5:4, similar to the ratio determined by

247   HPLC in glycolysis-inhibited sperm (Fig. 5, red lines). These results suggest that AK activity

248   may be so low that we can neglect its involvement in the energy transferring system in mouse

249   sperm under physiological conditions despite the presence of AK (Cao et al., 2006). Therefore,

250   in following calculations ANP profiles along the flagellum were done without AK activity (Fig.

251   5A-C).

252   When PGK activity was reduced to zero, drastic decrease was observed in ATP

253   concentration from 11.4 mmol l^{-1} (basal concentration) to 4.32 mmol l^{-1} and increase in ADP

254   concentration from 0.2 mmol l^{-1} (basal concentration) to 7.13 mmol l^{-1} at the tip of flagellum

255   were observed. The resultant activity of dynein ATPase at the tip of the flagellum attenuated

256   from 0.133 mmol l^{-1}/sec (basal value, this value is constant among calculations) to 0.0738

257   mmol l^{-1}/sec. The ATPase activity was calculated from the equation (2) in Materials and

258   Methods. This means that ATPase rate at the tip of the flagellum decreased to approximately

259   55% of the basal value.

260   When PGK reaction was included in the equation, a slight increase in ATP concentration

261   from 4.32 mmol l^{-1} to 4.5 mmol l^{-1} and a decrease in ADP concentration from 7.13 mmol l^{-1} to

262   7.0 mmol l^{-1} were observed in the presence of 0.155 mmol l^{-1} PGK substrates (total 3PG and 1,

263   3BPG). The resultant ATPase activity at the tip was 0.0754 mmol l^{-1}/sec, which is almost the

264 same to that calculated without the PGK activity. However, the ATPase activity at the tip of the

265 flagellum increased up to 0.0895 mmol l^{-1}/sec, 0.104 mmol l^{-1}/sec and 0.131 mmol l^{-1}/sec

266 when the concentration of the PGK substrates increased to 1.55 mmol l^{-1}, 3.1 mmol $l^{-1}$and 6.2

267 mmol l^{-1}, respectively (Fig. 5C). These results indicate that PGK has a capacity to transfer high

268 energy phosphoryls through spatial buffering of ATP when sufficient glycolytic intermediates

269 are available.

270

271

272

273

274

275

276

277

278

279 **Discussion**

280 Mammalian sperm must metabolize extracellular energy substrates to produce ATP for a

281 long period to accomplish fertilization. Recently, many investigators reported about the

282 relationship between metabolic pathway and flagellar motility in mouse sperm (Mukai and

283 Okuno, 2004; Miki et al., 2004; Ford, 2006; Tanaka et al., 2003), but none of them focused on

284 the different contribution of metabolic pathways to the flagellar movement. In the present

285 study, we performed detailed analysis of mouse sperm flagellar movement using various

286 parameters to estimate the difference of contribution of metabolic pathways to mouse sperm

287 motility, and revealed that glycolysis has an important role in energy transfer in mouse sperm

288 flagella.

289 As reported previously (Mukai and Okuno, 2004; Miki et al., 2004; Tanaka et al., 2003),

290 mouse sperm maintained vigorous motility for more than 60 min in the presence of energy

291 substrates (glucose, pyruvate, BHB). There was no difference in motility parameters (beat

292 frequency, bend angle, percentage of motility and sliding velocity) by substrates (Table 1).

293 Since glucose is metabolized by glycolysis alone when sufficient glucose is available (Odet et

294 al., 2011), these results indicate that mouse sperm are able to produce and supply sufficient

295 amount of ATP for maintaining motility by both glycolysis and respiration.

296 On the other hand, ACH, which inhibits GAPDH through oxidation in cytoplasm (Mohri

297 et al., 1975; Brown-Woodman et al., 1978; Stevenson and Jones, 1985), caused significant

298 decrease in the bend angle and the sliding velocity even in the presence of respiratory

299 substrates such as pyruvate or BHB (Fig. 1). Furthermore, measurements of local bending

300 revealed flagellar bending was severely inhibited by ACH and DOG especially at the distal

301 region of flagellum (Figs 2, 3). These results are inconsistent with the previous study (Tanaka

302 et al., 2004). Detailed analysis of flagellar movement of the present study allowed us to

303 evaluate motility change which had been overlooked in the assessments of the percentage of

304 motile sperm in the previous study.

305 If the beat frequency is assumed to be constant throughout the flagellum as Okuno and

306 Hiramoto (1976) suggested, a decrease in local bending at a distal part of flagellum indicates a

307 decrease in sliding velocity of doublet microtubule at that locus. Since the sliding velocity

308 correlates ATP concentration, the decreased bending suggests the decrease in ATP

309 concentration at the distal part of the flagellum in glycolysis-inhibited sperm. By contrast, it is

310 likely that ATP level at basal region of glycolysis-inhibited sperm is unchanged or almost

311 saturated since beat frequency and local bending of basal region was unaffected by ACH. This

312 motility character resembles in sea urchin sperm flagella in which the activity of creatine

313 kinase is inhibited. In this case, creatine phosphate and creatine kinase are indispensable for

314 energy supply from mitochondria located at basal region of flagellum to the distal end

315 (Tombes et al., 1987; Tombes and Shapiro, 1985). Moreover, Shingyoji and colleagues (1995)

316 reported about the relationship among the ATP concentration, beat frequency, bend angle and

317 sliding velocity using a head vibrating technique of demembranated sea urchin sperm as

318 follows; the head of demembranated sea urchin sperm suspended in a certain concentration of

319 ATP were held by suction at the tip of a micropipette and vibrated laterally with respect to

320 head axis. When sperm was vibrated at frequencies higher than undriven beat frequency of

321 flagella, the apparent time-averaged sliding velocity of axonemal microtubules remain

322 constant, with higher frequency being accompanied by decrease in the bend angle (Shingyoji

323 et al., 1995). This phenomenon corresponds with the present study; proximal region of flagella

324 is assumed to contain high concentration of ATP in the presence of respiratory substrates

325 because mitochondria are located at the proximal region of flagella (mid piece), resulting in

326 high sliding velocity therein. Generated bends propagate with a constant beat frequency to the

327 distal end of flagellum. However, decrease in ATP concentration at the distal end of flagellum

328 by glycolysis inhibition causes decrease in sliding velocity at distal end, as a consequence of

329 the decrease in bend angle. Taken together, glycolysis inhibition by ACH (or DOG) probably

330   induced a decrease in ATP, especially at the distal part of flagellum even in the presence of

331   respiratory substrates.

332   On the other hand, sperm swimming in the media supplied with respiration substrates

333   without glycolysis inhibition showed local bending and sliding velocity comparable to those

334   observed in sperm supplied with glucose throughout the flagellum. This result suggests

335   sufficient ATP was supplied to the distal end of flagellum. Taken together, it is likely that

336   glycolysis has an important role for the supply of ATP to the distal end of flagellum.

337   Since the decrease in ATP concentration at distal part of flagellum is assumed to result in

338   the decrease in total ATP in the sperm, total ATP in sperm was measured directly by

339   reversed-phase HPLC. As shown in Fig. 4, the total ATP content was apparently reduced by

340   ACH in pyruvate- and BHB-supplied sperm. By contrast, the ADP and AMP content increased

341   by ACH treatment. Because several mmol l^{-1} of ADP inhibits dynein ATPase in a competitive

342   manner (Okuno and Brokaw, 1979), the increase in ADP, together with the decrease in ATP

343   concentration, may impair microtubule sliding velocity. Therefore, it is likely that the

344   reduction in sliding velocity by inhibition of glycolysis may be induced by both decrease in

345   ATP and increase in ADP.

346   It was previously proposed that ATP produced in mitochondria at the base of flagellum is

347   supplied to the distal part of flagellum by simple diffusion (Nevo and Rikmenspoel, 1970).

348   Tombes and colleagues, however, reported that sea urchin sperm could not maintain normal

349   motility and failed in accomplishing fertilization without creatine kinase, an enzyme which

350   catalyzes the reaction that is indispensable for energy-transporting system (Tombes and

351   Shapiro, 1985; Tombes et al., 1987). Since mouse sperm have three times longer flagella (120

352   µm) than sea urchin sperm (40 µm), it is predicted that ATP produced in mitochondria at the

353   basal region of flagellum cannot be supplied sufficiently by simple diffusion. Nevertheless,

354   creatine kinase was not detected in mouse sperm (Kamp et al., 1996). Furthermore, knock out

355   of ubiquitous mitochondrial creatine kinase in mouse did not impact on sperm motility and

356   fertility (Steeghs et al., 1995). As mouse sperm apparently can supply adequate ATP from base

357   to the tip of the flagellum (Figs 2, 3), another energy supplying system in mouse sperm is

358   predicted.

359   In skeletal muscle, an energy transferring system by glycolytic enzymes through ATP

360   spatial buffering which is called near equilibrium enzymatic flux network, was proposed

361   recently (Dzeja et al., 2004; Dzeja and Terzic, 2003). In this system, individual glycolytic

362   enzymes work as an ATP spatial buffer, replenishing ATP at the distal part of the flagellum.

363   Sequential buffering reactions by glycolytic enzymes apparently "transfer" a wave of high

364   energy phosphoryls from basal mitochondria to the distal part of the flagellum. Based on their

365   theory, we would like to propose a hypothesis about a new function of glycolysis as energy

366   transferring system in mouse sperm flagella. Schematic model of energy transfer by glycolytic

367   enzymes is illustrated in Fig. 6. In this model, sequential rapid equilibrating reactions

368   catalyzed by phosphoglycerate kinase (PGK) and GAPDH work in concert as a spatial ATP

369   buffer, which transfer "energy wave" from the ATP producing site (mitochondria at mid-piece)

370   to ATP consuming sites (dynein arms along the flagellum) in the flagellum. To realize this ATP

371   spatial buffer, it is essential that enzymes involved in the reaction distribute throughout the

372   flagellum. From this point of view, glycolytic enzymes are suitable for supplying ATP since

373   glycolytic enzymes localize to the fibrous sheath as a complex, which runs along the entire

374   length of the sperm tail. In addition, it is assumed that reduction in the flagellar bending at the

375   distal part of the flagellum caused by ACH is attributed to the accumulation of Pi, a product of

376   ATP hydrolysis, because Pi acts as a competitive inhibitor as demonstrated in demembraneated

377   sea urchin sperm motility although the inhibition is not so strong (Okuno and Brokaw, 1979).

378   To validate the hypothesis that glycolytic enzyme functions as an ATP spatial buffer,

379   computer simulation of ANP diffusion along the flagellum was conducted based on the

380   algorithms by Tombes et al. (1987). In this simulation, we adopted the reaction by PGK only

381   since reaction of PGK is reported to be particularly important for transfer high energy

382   phosphoryls (Dzeja and Terzic, 2003). Although AK is abundantly present throughout the

383   mouse sperm flagella (Cao et al., 2006), we ignore the reaction of AK because of the reasons

384   described in Results.

385   The ATPase activity at the distal end attenuated from 0.133 mmol l^{-1}/sec (basal value) to

386   0.0738 mmol l^{-1}/sec in the absence of PGK reaction. Inclusion of the PGK activity did not

387   significantly cause the recovery of ATPase activity at the tip of the flagellum (0.0754 mmol

388   l^{-1}/sec) when the concentration of PGK substrates (total 3PG and 1, 3BPG) were 0.155 mmol

389   l^{-1}, a value determined by metabolomic analysis (Table 2). Increase in the concentration of

390   PGK substrates (~3.1 mmol l^{-1}), however, caused a recovery of ATPase activity to 0.104 mmol

391   l^{-1}/sec. Finally, ATPase activity at the tip did not decrease in the presence of PGK substrates as

392   high as 6.2 mmol l^{-1} (0.131 mmol l^{-1}/sec, Fig. 5). These results suggest that a PGK reaction

393   potentially acts as ATP spatial buffer, transferring energy in mouse sperm flagella when

394   sufficient PGK substrates are available. In *Lactococcus lactis*, more than 10 mmol l^{-1} of 3PG

395   was observed by ^{13}C-NMR analysis (Neves et al., 2000). In addition, 3PG and 1, 3BPG

396 concentrations in mouse brain cells were calculated to be 18.4 and 20.8 mmol l^{-1}, respectively,

397 by computer simulation analysis (Olán et al., 2008). By contrast to these reports, PGK

398 substrates concentration determined by metabolomic analysis in the present experiment was

399 much lower, 0.155 mmol l^{-1} (Table 2). Since 3PG and 1, 3BPG are highly unstable compounds,

400 it could be speculated that they have been degraded during sample preparation in the present

401 experiment, resulting in underestimation of the concentration of PGK substrates. The actual

402 concentrations of PGK substrates could be enough for energy transfer in mouse sperm.

403 The calculated ratio of the total intraflagellar ATP to the total ADP in the presence of 1.55

404 mmol l^{-1} PGK substrates was 5:2. The ratio of total intracellular ATP to total ADP in

405 glycolysis-non-inhibited sperm determined by HPLC measurements in the present experiments

406 represented 5:2-6:2 (Fig. 4). This ratio, 5:2, is obtained by simulation when PGK concentration

407 is 1.55 mmol l^{-1}. Therefore, the experimental data seems to support that actual value of

408 intracellular PGK substrates are approximately 1.55 mmol l^{-1}.

409 On the other hand, fitting of the results of computer simulation to the results of flagellar

410 movement analysis suggested a different concentration of PGK substrates. The ATPase activity

411 at the tip of the flagellum calculated from the PGK activity in the presence of 6.2 mmol l^{-1}

412 PGK substrates was 0.131 mmol l^{-1}/sec. By contrast, The ATPase activity at the tip of the

413 flagellum without PGK activity was 0.0738 mmol l^{-1}/sec; the ratio between two ATPase values

414 was 0.56. This ratio was similar to the ratio of local bending of glycolysis-inhibited sperm to

415 that of control sperm at the tip of the flagellum, which was approximately 0.5 (see Figs 2, 3).

416 Changes in local bending along the flagellum in the presence of ACH obtained in the present

417 experiments (Fig. 2C and D) and the simulated ATPase activity (Fig. 5C) are superimposed in

418   Fig. 7. The relatively good coincidence of them suggests that the energy transporting system

419   by means of glycolysis could be employed in the flagellum. These results suggest that realistic

420   intracellular concentration of PGK substrates is approximately 6.2 mmol l^{-1}. Taken together,

421   the concentration of PGK substrates were assumed to be 1.5-6.2 mmol l^{-1}. Under present

422   experimental conditions, such concentrations of PGK substrates might realized by high

423   concentrations of respiratory substrates which would stop glycolytic flux, or alternatively high

424   concentrations of respiratory substrates would replenish PGK substrates by reverse reaction

425   that are conventionally considered irreversible under physiological condition. Although the

426   results from computer simulation analysis strongly suggest that PGK has a potential to

427   functions as ATP spatial buffer, transferring energy in mouse sperm flagella, further studies to

428   determine the accurate value of PGK substrates concentration are necessary.

429   In conclusion, it was suggested that the ATP content in distal part of flagellum is reduced

430   by glycolysis inhibition even in the presence of substrates of respiration. Based on this result,

431   we proposed a new energy transfer system based on spatial buffering of ATP by glycolytic

432   enzymes in mouse sperm. Further investigations about this new function of glycolysis in

433   mouse sperm are needed, and would shed a light on energy homeostasis not only in

434   mammalian sperm physiology, but also in diverse motile cilia and flagella.

435

436

437

438

439

Materials and Methods

Sperm preparation

Sperm were obtained from the cauda epididymis of 8-15 wk old ICR male mice (*Mus Musculus*) in accordance with the guidance of the University of Tokyo. The cauda epididymis was excised and punched with needles. Epididymal sperm was gently squeezed out and diluted into 100 µl of sucrose solution (300 mmol l^{-1} sucrose, 10 mmol l^{-1} Hepes-NaOH, pH 7.4), in which sperm exhibited very low activity (about 1 Hz of beat frequency), referred to as the initiated sperm by Fujinoki et al (2001). The sperm suspension was diluted with the test solution for the following experiments. The test solution contains 150 mmol l^{-1} NaCl, 5.5 mmol l^{-1} KCl, 0.4 mmol l^{-1} $MgSO_4$, 1 mmol l^{-1} $CaCl_2$, 10 mmol l^{-1} $NaHCO_3$, 10 mmol l^{-1} Hepes-NaOH (pH 7.4), and 10 mmol l^{-1} of metabolic substrates, such as glucose (Glc), pyruvate (Pyr), and BHB. One volume of sperm suspension was diluted into 20 volume of each test solution and was incubated in CO_2 incubator (37℃, 5% CO_2) for observation.

For the inhibition of glycolysis, either 10 mmol l^{-1} of ACH or 10 mmol l^{-1} of DOG was added to each test solution.

Analysis of sperm motility

After the incubation in the test solution containing metabolic substrates and inhibitors, an aliquot of sperm suspension was placed onto a prewarmed glass slide at 37℃ and covered with a coverslip for observation with a microscope.

For the analysis of microtubule sliding velocity, sperm with their head attach to the glass surface was observed using a phase-contrast microscope (Diaphoto, Nikon, Tokyo, Japan), captured by a CCD camera (CR-20, Video Device, Chiba, Japan) and recorded by a video

462   recorder (HR-G11, Victor・JVC, Kanagawa, Japan). To analyze the sliding velocity, the

463   flagellar waveforms were carefully traced by hand from a video monitor onto a transparent

464   plastic film. The beat frequency was calculated from the number of video fields required to

465   complete one beat cycle determined by using the traced waveform. The bend angle of a

466   flagellum was determined by measuring the angle between the tangents at two adjacent point

467   of inflection when flagellar bends reach at the center of flagellum (Fig. 8A). Bend angle was

468   measured for both principal bends (Fig. 8A-a) and reverse bends (Fig. 8A-b), and data were

469   expressed as a sum of both values. Microtubule sliding velocity was defined as the

470   multiplication of beat frequency and bend angle.

471   For the measurement of the shear angle, sperm with their head attached to the glass

472   surface was recorded digitally using a phase-contrast microscope and a computer-driven

473   high-speed camera (HAS-220CH, DITECT, Tokyo, Japan). The shear angle of sperm flagella

474   was analyzed by "Bohboh", a flagellar movement auto-analyzing software kindly provided by

475   Dr. Shoji Baba (emeritus professor at Ochanomizu University, Tokyo, Japan). Shear angle was

476   defined as the angle between the reference line at the base of the flagellum, usually parallel to

477   the head axis, and the tangent at a point along the flagellum (See Fig. 8B). In the present

478   experiment, shear angle was determined every 10 µm on the flagellum from the base to the tip

479   for 3 cycle of beating. Then, difference between the maximum and minimum values was

480   defined as a local amount of microtubule sliding per one beat cycle (Fig. 8B).

481   A local bend angle, defined as the angle between the tangents at the two inflection points

482   around each vertex of the waveform, was determined on the images captured digitally by

483   high-speed camera. The analysis was conducted manually as the determination of bend angle.

484   The distance of bending vertex from the base of flagellum was determined digitally by Bohboh

485   software.

Measurement of ATP content by reversed phase HPLC

487   Evaluation of ATP content in mouse sperm cells was performed by reversed-phase HPLC

488   (LC10VP series, Shimadzu, Kyoto, Japan) with slight modifications (Mukai and Okuno, 2004;

489   Samizo et al., 2001). Sperm suspended with each test solution in microtubes were incubated in

490   a CO_2 incubator (5% CO_2, 37℃) for 30 min. One-tenth volume of 3% ice chilled perchloric

491   acid (PCA) was added to each sperm suspension to remove proteins, and the microtubes were

492   placed on ice for 10 min. After centrifugation (10000 x g, 10 min, 4℃), the supernatant was

493   filtered with a membrane of 0.22 µm pore size. Filtered solution was neutralized with

494   phosphate buffer, and 25 µl of neutralized solution was applied to a reversed-phase HPLC

495   column (Phenomenex Luna 5 µC18, 4.6 × 150 mm; Shimadzu GLC, Tokyo, Japan). The

496   mobile phase contained 20 mmol l^{-1} potassium phosphate (pH 6.8), and 5 mmol l^{-1} of

497   tetrabutyl-ammonium hydroxide, and 20% methanol. The number of sperm cells was counted

498   in each sample, and the content of ATP was represented as nmol per 10^6 sperm.

Metabolomic analysis

500   To determine the content of glycolytic intermediates, metabolome analysis was performed

501   by a capillary electrophoresis electrospray ionization time-of-flight mass spectrometry

502   (CE-TOFMS) method. One ml of sperm suspension in sucrose solution was diluted into

503   10-fold volumes of each test solution containing 1 mmol l^{-1} glucose or 10 mmol l^{-1} pyruvate

504   with or without 10 mmol l^{-1} ACH, and incubated for 30 minutes at 37℃. After incubation,

505   75% percoll was added to the bottom of the tube and centrifuged for 5 minutes at 900 x g, 4℃.

506   Sperm were observed in the layer between the test solution and percoll. Then the supernatant

507   test solution was discarded and the resultant was washed with 5% (w/w) mannitol solution to

508   remove electrolytes. After centrifugation (900 $\times$ g, 4℃, 2.5 minutes), supernatant was

509   discarded and 1 ml of ice-cold methanol was added to fix sperm. Methanol-fixed sperm

510   samples were separated by capillary electrophoresis and the amount of each intermediates are

511   quantified by Mass spectrometry. CE-TOFMS analysis was performed by Human Metabolome

512   Technologies Inc.(Yamagata, Japan).

513   ***Computer simulation analysis of diffusion of ATP and high energy phosphoryls***

514   Calculation of high energy phosphoryls diffusion along the flagellum is performed based

515   on the algorithms previously reported by Tombes et al (1987). In the model, each molecular

516   species diffusing along the flagellum is governed by a diffusion equation,

517

$$\frac{\partial C_{(s,t)}}{\partial t} = D \cdot \frac{\partial^2 C_{(s,t)}}{\partial s^2} + Q_{(s,t)} \quad \cdots\cdots\cdots\cdots\cdots\cdots\cdots\cdots (1)$$

518   where $C_{(s,\,t)}$ represents the concentration of the diffusing species at position s and time t. D is

519   the relevant diffusion coefficient, and Q is the rate of production of the species by chemical

520   reactions. Q consisted of three reactions, specified by Q_1, Q_2 and Q_3, are described below.

521   Q_1 is the dynein ATPase rate. Since the use of ATP by flagella is tightly coupled to

522   motility, the relationship between the ATPase rate and the ATP concentration is assumed to be

523   similar to the relationship between flagellar beat frequency and ATP concentration.

524

$$Q_1 = Q_{1F} \Big/ \left(1 + K1 \left(1 + \frac{[ADP]}{K_i} \Big/ [ATP] \right) \right) \quad \cdots\cdots\cdots\cdots\cdots\cdots\cdots (2)$$

525   where K1 is the ATP concentration for half-maximal beat frequency, and Ki is the

526   constant for competitive inhibition of ATPase rate (beat frequency) by ADP. The maximum

527   rate, Q_{1F}, obtained as value of 0.134 mmol l^{-1}/sec, based on measurements of glucose

528   consumption by mouse sperm with the assumption that glucose is metabolized only by

529   glycolysis (Odet et al., 2011). K1 value of 0.14 mmol l^{-1}, obtained from the measurements on

530   demembranated ram sperm, was kindly provided by Dr. Sumio Ishijima (Tokyo Institute of

531   Technology). A value of 0.28 mmol l^{-1} was used for Ki, based on the measurements indicating

532   that the value of Ki for demembranated sea urchin sperm flagella was twice the value of K1

533   (Okuno and Brokaw, 1979). The reverse reaction for the ATPase is neglected.

534   Q_2 is the rate for the glycolytic reactions. Because enzyme that catalyze the first step of

535   ATP producing reaction (PGK) is reported to be particularly important for transferring high

536   energy phosphoryls (Dzeja et al., 2004), only the reaction by PGK is included. This may be a

537   good assumption, as glycolytic enzymes exist in a complex manner in spermatozoa (Westhoff

538   and Kamp, 1997). The reaction by PGK is as follows:

539        $$ATP + 3PG \rightarrow ADP + 1,3BPG \quad \cdots\cdots\cdots\cdots\cdots\cdots\cdots\cdots\cdots (3)$$

540   where 3PG represents 3-phosphoglycerate and 1, 3BPG represents 1, 3-bisphosphoglycerate.

541   For this reaction, both forward and reverse rates are considered;

542    $$Q_2 = \left(Q_{2F} \frac{[3PG][ATP]}{K_{mP}K_{mT}} - Q_{2R} \frac{[1,3BPG][ADP]}{K_{mB}K_{mD}} \right) \Bigg/ \left(1 + \frac{[3PG][ATP]}{K_{mP}K_{mT}} + \frac{[1,3BPG][ADP]}{K_{mB}K_{mD}} + \frac{[ATP]}{K_{mT}} + \frac{[3PG]}{K_{mP}} + \frac{[1,3BPG]}{K_{mB}} + \frac{[ADP]}{K_{mD}} \right)$$

543        $$\cdots\cdots\cdots\cdots\cdots\cdots\cdots\cdots (4)$$

544   Values used for the parameters in this equation are given in Table 2.

545   Q_3 is the rate for the adenylate kinase (Noda, 1973).

546        $$ATP + AMP \rightarrow 2ADP \quad \cdots\cdots\cdots\cdots\cdots\cdots\cdots\cdots\cdots (5)$$
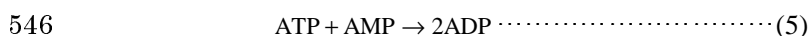
547   For   this   reaction   also,   both   forward   and   reverse   rates   are   considered.

548
$$Q_3 = \left(Q_{3F} \frac{[ATP][AMP]}{K_N K_M} - Q_{3R} \frac{[ADP][AMP]}{K_A K_A} \right) \Bigg/ \left(1 + \frac{[ATP][AMP]}{K_N K_M} + \frac{[ADP][ADP]}{K_A K_A} + \frac{[ATP]}{K_N} + \frac{[AMP]}{K_M} + \frac{2[ADP]}{K_A} \right)$$

549 $\cdots\cdots\cdots\cdots\cdots\cdots\cdots\cdots$ (6)

550 The parameters used to calculate in this equation (Q_{3F}, Q_{3R}, K_N, K_M, K_A), which are originated

551 from rabbit muscle fiber, are given in Table 2.

552 For each species, Q is the sum of the relevant rates as follows: For ATP: $Q = -Q_1 - Q_2 - Q_3$,

553 for ADP: $Q = Q_1 + Q_2 + 2Q_3$, for AMP: $Q = -Q_3$, for 3PG: $Q = -Q_2$, for 1, 3BPG: $Q = Q_2$.

554 If the diffusion coefficients for ATP, ADP, and AMP and those for 3PG and 1, 3BPG are

555 assumed to be almost equivalent, there will be no gradient of total adenine nucleotide or total

556 3PG concentration along the flagellum. Thus, AMP can be obtained from (total adenine

557 nucleotide – ATP – ADP) and 3PG can be obtained from (3PG + 1, 3BPG) — 1, 3BPG.

558 To solve the system of partial differential equations, three equations were integrated

559 forward with time until a steady equilibrium solution was obtained. Concentrations at the basal

560 end of the flagellum were held constant, and no fluxes were allowed past the distal end of the

561 flagellum. Then, for each species, equation (1) was converted to

562
$$C_{(s,t+\Delta t)} = C_{(s,t)} + D \left[\left(C_{(s-\Delta s,t)} - 2C_{(s,t)} + C_{(s+\Delta s,t)} \right) \Big/ \Delta s^2 \right] \Delta t + Q_{(s,t)} \bullet \Delta t \quad \cdots\cdots\cdots\cdots (7)$$

563 The length interval, Δs, was 1 µm in all the results shown, and the time interval, Δt, was

564 normally 0.5 msec. The simulation program was written and performed by computer

565 software Mathematica (Wolfram Research, Champaign, IL, USA).

566

567 *Statistical analysis*

568   Values for sliding velocity, shear angle, and ATP content were expressed as the mean and

569   standard error of the measure (s. e. m.). Statistical tests were performed using Student's t-test

570   for testing differences of content of adenine nucleotides. In the other experiments, data were

571   analyzed by ANOVA and post-hoc Tukey-Kramer test.

572   ***Reagents***

573   α-chlorohydrin was purchased from Sigma-Aldrich (St. Louis, U.S.A.),

574   β-hydroxybutyrate was from MP Biomedicals (California, U.S.A.), percoll was from GE

575   Healthcare (Chalfont St Giles, UK.), and the other chemicals were purchased form Wako Pure

576   Chemicals Co. ltd. (Osaka, Japan).

587

588   **Abbreviations**

589   ACH: α- chlorohydrin

590   ADP: adenosine diphosphate

591   AMP: adenosine monophosphate

592   ATP: adenosine triphosphate

593   BHB: β-hydroxy butyrate

594   1, 3-BPG: 1, 3-bisphosphoglycerate

595   DOG: 2-deoxy-D-glucose

596   GAP: glyceraldehyde-3-phosphate

597   GAPDH: glyceraldehyde-3-phosphate dehydrogenase

598   GAPDS: glyceraldehyde-3-phosphate dehydrogenase, spermatogenic

599   Glc: glucose

600   3PG: 3-phosphoglycerate

601   PGK: phosphoglycerate kinase

602   Pi: inorganic phosphate

603

604

605

606

607

608

609

610

611

612 **Figure legends**

613 Figure 1: Effect of ACH on sperm flagellar motility in the presence of various substrates.

614 Sperm was diluted into the media containing substrates only or substrates and inhibitor. Then,

615 change in beat frequency (A), bend angle (B) and shear angle (C) with time-course was plotted.

616 Both the shear angle and the bend angle are represented as the averaged absolute values obtained

617 from both the principal and reverse bend. Beat frequency was not significantly reduced by ACH

618 when pyruvate or BHB was present in the media. By contrast, bend angles and shear angles were

619 significantly reduced by ACH even when pyruvate or BHB was present in the media.

620 Concentrations of substrates and inhibitor were 10 mM. Vertical bars represent SEM. N>9 Asterisks

621 indicate significant difference from control sperm (*: $p<0.05$, **: $p<0.01$). Glc: glucose, Pyr:

622 pyruvate. ACH: α-chlorohydrin

623

624 Figure 2: Changes of local bending along the glycolysis-inhibited sperm flagella

625 Sperm were diluted into media containing respiration substrates (A: BHB; B: Pyr) and

626 glycolysis inhibitor (ACH or DOG), then allowed to swim in the media for 1 hour in a CO_2

627 incubator (37℃, 5% CO_2, 95% air). After incubation, local shear angle was measured with

628 computer software Bohboh. Changes of shear angle are plotted at indicated distance from the head

629 (A, B). Data shown in (A, B) were expressed as the ratio of the shear angle in control to that in the

630 glycolysis-inhibited sperm (C, D). Bending decreases in the distal part of flagellum. The

631 concentration of each substrate and inhibitor was 10 mM. Bars represent SEM. N=5. Asterisks

632 indicate significant difference from control sperm (*: $p<0.05$, **: $p<0.01$).

633

634   Figure 3: Scattergram of typical changes of local bend angle with the length of flagella

635   Sperm diluted into media containing respiration substrates and glycolysis inhibitor (ACH), then

636   allowed to swim in the media for 1 hour in a CO_2 incubator (37℃, 5%CO_2, 95% air). After

637   incubation, local bend angle was determined for flagella of sperm attached to the glass surface by

638   the head. Measurement was performed as described in Materials and methods. Data are shown as

639   scattergram. ACH-treated sperm (open characters) showed reduced bend angles compared with

640   non-treated controls (filled characters). The concentrations of each substrate and inhibitor were 10

641   mM.

642   Glc: glucose, Pyr: pyruvate. ACH: α-chlorohydrin

643

644   Figure 4: Effect of glycolytic inhibitor on the content of ANP in sperm.

645   Content of ANPs are measured by Reversed-phase HPLC 30 minutes after activation. Decrease

646   in the ATP content and increase in the ADP and AMP contents by ACH were observed even in the

647   presence of respiratory substrates. The concentration of each substrate and inhibitor was 10 mM.

648   Data are means of 15 mice ±SEM. Asterisks indicate significant difference from control sperm (*:

649        $p<0.05$, **: $p<0.01$).

650   Glc: glucose, Pyr: pyruvate. ACH: α-chlorohydrin

651

652   Figure 5: Simulation of high energy phosphoryls diffusion along the flagellum.

653   Calculated concentration profiles of ATP (A) and ADP (B), and calculated profiles of ATPase

654   activity (C) without adenylate kinase activity using the parameters given in Table 2 and equation

655   indicated by Tombes et al. (1987) are shown.

656

657   Figure 6: Schematic model of energy transfer system by glycolysis

658   Schematic models of energy transporting system in sperm flagella by glycolysis is illustrated

659   by modifying energy transfer system proposed by Dzeja and Terzic (2003) to sperm flagella.

660   PGK: phosphoglycerate kinase

661   GAPDS: glyceraldehyde-3-phosphate dehydrogenase, spermatogenic

662   GAP: glyceraldehyde-3-phosphate

663   3PG: 3-phosphoglycerate

664   1, 3-BPG: 1, 3-bisphosphoglycerate

665   NAD: nicotinamide adenine dinucleotide (oxidized)

666   NADH: nicotinamide adenine dinucleotide (reduced)

667   Pi: inorganic phosphate

668

669   Figure 7: Superimposed schematic model of energy transporting system without glycolysis to the

670   flagellar local bending inhibited by ACH

671   Simulated ATPase activity along flagellar axis in the absence of energy transporting system by

672   glycolysis (Fig. 6C) is superimposed to the relative change in flagellar local bending when

673   glycolysis is inhibited by ACH. Results from BHB + ACH (Fig. 3 C) and Pyruvate + ACH (Fig. 3

674   D) are averaged.

675

676   Figure 8: Methods for analysis of flagellar movement.

677   (A) Analysis of bend angle. The bend angle of a flagellum was determined as follows: First,

678 measuring the angle between the tangents at two adjacent inflection points when flagellar bends

679 reach at the center of flagellum (white circle). The angle was measured for both principal bends (a)

680 and reverse bends (b), and bend angle is defined as a sum of both values. The bend angle was

681 measured three times individually, and the bend angle of each spermatozoon was determined as a

682 mean of them.

683   (B) Analysis of shear angle. Shear angle at point c in left picture was defined as the angle

684 between the reference line at the base of the flagellum, usually parallel to the head axis, and the

685 tangent at a point c. In the present experiment, shear angle was determined every 10 µm on the

686 flagellum from the base to the tip for 3 cycle of beating (plotted in right graph). Then, difference

687 between the maximum and minimum values (arrows in right graph) was defined as a local amount

688 of microtubule sliding.

689

690

691

692

693

694

695

696

697

698

699

References

Austin, C. R. (1985). Sperm maturation in the male and female genital tracts. In: *Biology of Fertilization vol. 2: Biology of the Sperm* (ed. C. B. Metz and A. Monroy), pp. 121-155. New York: Academic Press.

Brown-Woodman, P. D. C., Mohri, H., Mohri, T., Suter, D. and White, I. G. (1978). Mode of action of α-chlorohdrin as a male anti-fertility agent. *Biochem. J.* **170**, 23-37.

Cao, W., Haig-Ladewig, L., Gerton, G. L. and Moss, S. B. (2006). Adenylate kinase 1 and 2 are part of accessory structures in the mouse sperm flagellum. *Biol. Reprod.* **75**, 492-500.

Danshina, P. V., Geyer, C. B., Dai, Q., Goulding, E. H., Willis, W. D., Kitto, G. B., McCartney, J. R., Eddy, E. M. and O'Brien, D. A. (2010). Phosphoglycerate kinase 2 (PGK2) is essential for sperm function and male fertility in mice. *Biol. Reprod*. **82**, 136-145.

Dzeja, P. and Terzic, A. (2003). Phosphotransfer networks and cellular energetic. *J. Exp. Biol.* **206**, 2039-2047

Dzeja, P., Terzic, A. and Wieringa, B. (2004). Phosphotransfer dynamics in skeletal muscle from creatine kinase gene-deleted mice. *Mol. Cell Biochem.* **256/257**, 13–27.

Ford, W. C. L. (2006). Glycolysis and sperm motility: does a spoonful of sugar help the flagellum go round? *Hum. Reprod. Update.* **12**, 269-274.

Ford, W. C. L. and Harrison, A. (1985). The presence of glucose increases the lethal effect of a-chlorohydrin on ram and boar spermatozoa in vitro. *J. Reprod. Fertil.* **73**,197–206.

Ford WCL and Harrison A. (1986). The concerted effect of alpha-chlorohydrin and glucose on the ATP concentration in spermatozoa is associated with the accumulation of glycolytic intermediates. *J. Reprod. Fertil.* **77**, 537–545.

722 **Fujinoki, M., Ohtake, H. and Okuno, M.** (2001). Serine phosphorylation of flagellar

723 proteins associated with the motility activation of hamster spermatozoa. *Biomed. Res.* **22**,

724 45–58.

725 **Hiipakka, R. A. and Hammerstedt, R. H.** (1978). 2-Deoxylucose transport and

726 phosphorylation by bovine sperm. *Biol. Reprod.* **19**, 368-379.

727 **Hyne, R. V. and Edwards, K. P.** (1985). Influence of 2-deoxy-D-glucose and energy

728 substrates on guinea pig sperm capacitation and acrosome reaction. *J. Reprod. Fertil.* **73**,

729 59-69.

730 **Kamp, G., Busselmann, G. and Lauterwein, J.** (1996). Spermatozoa: models for studying

731 regulatory aspects of energy metabolism. *Experientia*. **52**, 487-494

732 **Krisfalusi, M., Miki, K., Magyar, P. L. and O'Brien, D. A.** (2006). Multiple Glycolytic

733 Enzymes Are Tightly Bound to the Fibrous Sheath of Mouse Spermatozoa. *Biol. Reprod.* **75**,

734 270-278.

735 **Miki, K., Qu, W., Goulding, E. H., Willis, W. D., Bunch, D. O., Strader, L. F, Perreault,**

736 **S. D., Eddy, E. M. and O'Brien, D. A.** (2004). Glyceraldehyde 3- phosphate

737 dehydrogenase-S, a sperm specific glycolytic enzyme, is required for sperm motility and male

738 fertility. *Proc. Natl. Acad. Sci.* **101**, 16501-16506.

739 **Mohri, H., Suter, D. A. I., Brown-Woodman, P. D. C, White, I. G. and Ridley, D. D.**

740 (1975). Identification of the biochemical lesion produced by α-chlorohydrin in spermatozoa.

741 *Nature* **255**, 75-77.

742 **Mukai, C. and Okuno, M.** (2004). Glycolysis plays a major role for adenosine triphosphate

743 supplementation in mouse sperm flagellar movement. *Biol. Reprod.* **71**, 540-547.

744   **Neves, A. R., Ramos, A., Shearman, C., Gasson, M. J., Almeida, J. S. and Santos, H.**

745   (2000). Metabolic characterization of *Lactococcus lactis* deficient in lactate dehydrogenase

746   using in vivo ^{13}C-NMR. *Eur. J. Biochem.* **267**, 3859-3868.

747   **Nevo, A. C. and Rikmenspoel, R.** (1970). Diffusion of ATP in sperm flagella. *J. Theor. Biol.*

748   **26**, 11-18

749   **Noda L.** (1973). Adenylate kinase In *The Enzymes: Vol. VIII.* (ed. P. D. Boyer), pp. 279-305.

750   New York: Academic Press.

751   **Odet, F., Duan, C., Willis, W. D., Goulding, E. H., Kung, A., Eddy, E. M. and O'Brien,**

752   **D. A.** (2008). Expression of the gene for mouse lactate dehydrogenase C (Ldhc) is required for

753   male fertility. *Biol. Reprod.* **79**, 26-34.

754   **Odet, F., Gabel, S. A., Williams, J., London, R. E., Gouldberg, E., Kung, A. and Eddy,**

755   **E. M.** (2011). Lactate dehydrogenase C (LDHC) and energy metabolism in mouse sperm. *Biol.*

756   *Reprod.* **85**, 556–564

757   **Okuno, M. and Hiramoto, Y.** (1976). Mechanical stimulation of starfish sperm flagella. *J.*

758   *Exp. Biol.* **65,** 401-413.

759   **Okuno, M. and Brokaw, C. J.** (1979). Inhibition of movement of triton-demembranated

760   sea-urchin sperm flagella by Mg^{2+}, ATP^{4-}, ADP and Pi. *J. Cell Sci.* **38**, 105-123.

761   **Olán, J., Klivényi, P., Gardián, G., Vécsei, L., Orosz, F., Kovacs, G. G., Westerhoff, H.**

762   **V. and Ovádi, J.** (2008). Increased glucose metabolism and ATP level in brain tissue of

763   Huntington's disease transgenic mice. *FEBS J.* **275**, 4740-4755.

764   **Pegoraro, B. and Lee, C. Y.** (1978). Purification and characterization of two iozymes of

765   3-phosphoglycerate kinase from the mouse. *Biochim. Biophys. Acta* **522**, 423-433

766   **Samizo, K., Ishikawa, R., Nakamura, A. and Kohama, K.** (2001). A highly sensitive

767   method for measurement of Myosin ATPase activity by Reversed-phase high performance

768   liquid chromatography. *Anal. Biochem.* **293**, 212-215.

769   **Shingyoji, C., Yoshimura, K., Eshel, D., Takahashi, K. and Gibbons, I. R.** (1995). Effect

770   of beat frequency of microtubule sliding in reactivates sea urchin sperm flagella under

771   imposed head vibration. *J. Exp. Biol.* **198**, 645-653

772   **Si, Y. and Okuno, M.** (1995). Activation of mammalian sperm motility by regulation of

773   microtubule sliding via cyclic adenosine 5'-monophosphate-depemdent phosphorylation. *Biol.*

774   *Reprod.* **53**, 1081-1087.

775   **Steeghs, K., Oerlemans, F. and Wieringa. B.** (1995). Mice deficient in ubiquitous

776   mitochondrial creatine kinase are viable and fertile. *Biochim. Biophys. Acta* **1230**, 130-138

777   **Stevenson, D. and Jones, A. R.** (1985). Production of (S)-3-chlorolactaldehyde from

778   (S)-α-chlorohydrin by boar spermatozoa and the inhibition of glyceraldehydes 3-phosphate

779   dehydrogenase in vitro. *J. Reprod. Fert.* **74**, 157-165

780   **Takao, D. and Kamimura, S.** (2008). FRAP analysis of molecular diffusion inside

781   sea-urchin spermatozoa. *J. Exp. Biol.* **211**, 3594-3600

782   **Tanaka, H., Takahashi, T., Iguchi, N., Kitamura, K., Miyagawa, Y., Tsujimura, A.,**

783   **Matsumiya, K., Okuyama, A. and Nishimune, Y.** (2004). Ketone bodies could support the

784   motility but not the acrosome reaction of mouse sperm. *Int. J. Androl.* **27**, 172-177.

785   **Tombes, R. M. and Shapiro, B. M.** (1985). Metabolite channelling: a phosphoryl creatine

786   shuttle to mediate high energy phosphate transport between sperm mitochondrion and tail. *Cell*

787   **41**, 325-334

788   **Tombes, R. M., Brokaw, C. J. and Shapiro, B. M.** (1987). Creatine kinase-dependent

789   energy transport in sea urchin spermatozoa. *Biophys. J.* **52**, 75-86

790   **Welch, J. E., Brown, P. L., O'Brien, D. A., Magyar, P. L., Bunch, D. O., Mori, C. and**

791   **Eddy, E. M.** (2000). Human glyceraldehydes 3-phosphate dehydrogenase-2 gene is expressed

792   specifically in spermatogenic cells. *Int. J. Androl.* **21**, 328-338

793   **Westhoff, D. and Kamp, G**. (1995). Glyceraldehyde 3-phosphate dehydrogenase is bound

794   to the fibrous sheath of mammalian spermatozoa. *J. Cell Sci.* **110**, 1821-1829

795   **Wolfgang, K. G. K. and Theodor, B.** (1970). 3- phosphoglycerate kinase from rabbit

796   skeletal muscle and yeast. *Eur. J. Biochem.* **17**, 568-580

797   **Yano, Y. and Miki, N. T.** (1980). Sliding velocity between outer doublet microtubules of

798   sea-urchin sperm axonemes. *J. Cell Sci.* **44**, 169-186.

799   **Yeung, C. H., Anapolski, M. and Cooper, T.** (2002). Measurement of volume changes in

800   mouse spermatozoa using an electronic sizing analyzer and a flow cytometer: validation and

801   application to an infertile mouse model. *J. Androl.* **23**, 522-528.

802

803

804

805

806

807

808

809

810   **Tables**

811

812   Table 1. Difference of beat frequency, bend angle, sliding velocity and waveform of sperm

813   flagella depends on energy substrates.

	Glc n=16	Pyr n=9	BHB n=17
Beat Frequency (Hz)	16.3±0.70	14.6±0.72	16.9±1.13
Bend Angle (rad)	2.55±0.12	2.62±0.07	2.63±0.16
Sliding Velocity (rad/sec)	41.0±1.91	38.1±1.60	42.6±2.26
Motility (%)	55.8±4.60	58.8±2.43	56.3±3.92
Waveform			

814

815   Difference in beat frequency, bend angle, sliding velocity, percentage of motile sperm and typical

816   waveform by substrates are indicated. Data are represented as mean value ± s. e. m. No

817   significant difference in motility parameters was recognized. Concentration of substrates was

818   10 mmol l^{-1}.

819

820

821   Table 2. Parameters used for computations of Pi transport in flagella

Parameters	Value	Reference
Flagellar length	100 µm	See text
Diffusion coefficient for ANP	60 $\mu m^2 s^{-1}$	Takao and Kamimura (2008)
Diffusion coefficient for 3PG and 1, 3 BPG	104 $\mu m^2 s^{-1}$	Same as above
PGK substrates concentration (Total 3PG and 1, 3BPG)	0.155 mmol l^{-1}	Determined by metabolomic analysis
Total adenine nucleotide	11.6 mmol l^{-1}	Same as above
Q_{1F}	0.134 mmol l^{-1}/sec	Odet et al (2011)
Kl (K_m of ATPase from ATP, from ATP concentration for half-maximal beat frequency of demembranated flagella)	0.14 mmol l^{-1}	Ishijima, personal data
K_i (for inhibition of flagellar beat frequency by ADP)	0.28 mmol l^{-1}	Okuno and Brokaw (1979)
K_{mP} (PGK2 K_m value for 3PG)	1.55 mmol l^{-1}	Pegoraro and Lee (1978) Wolfgang and Theodor (1970)
K_{mT} (PGK2 K_m value for ATP)	0.32 mmol l^{-1}	Same as above
K_{mB} (PGK2 K_m value for 1, 3BPG)	0.0022 mmol l^{-1}	Same as above
K_{mD} (PGK2 K_m value for ADP)	0.16 mmol l^{-1}	Same as above
Q_{2R}/Q_{2F} (ratio of reverse to forward PGK2)	2.71	Same as above
K_A (myokinase K_m value for ATP)	0.3 mmol l^{-1}	Noda, (1973) [23]
K_N (myokinase K_m value for ADP)	0.3 mmol l^{-1}	Same as above
K_M (myokinase K_m value for AMP)	0.3 mmol l^{-1}	Same as above
Q_{3R}/Q_{3F} (ratio of reverse to forward adenylate kinase)	1.0	Same as above
Cytosolic volume	53.5 fL	Yeung et al., (2002) [40]

822

823

824

825   **Figures**

826   (A)   Beat frequency
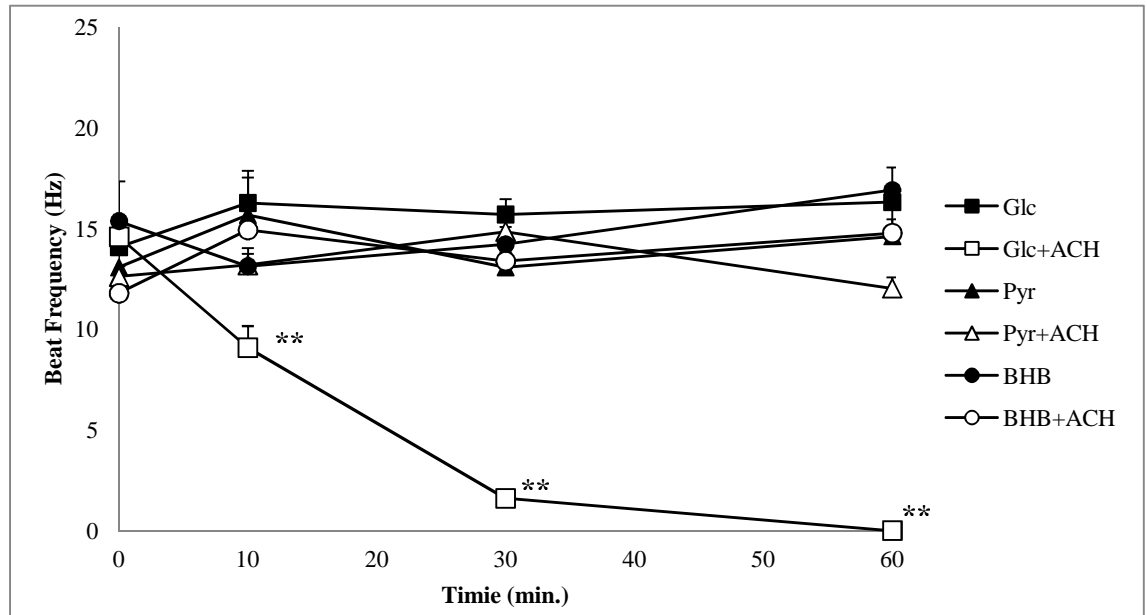
827

828   (B)   Bend angle
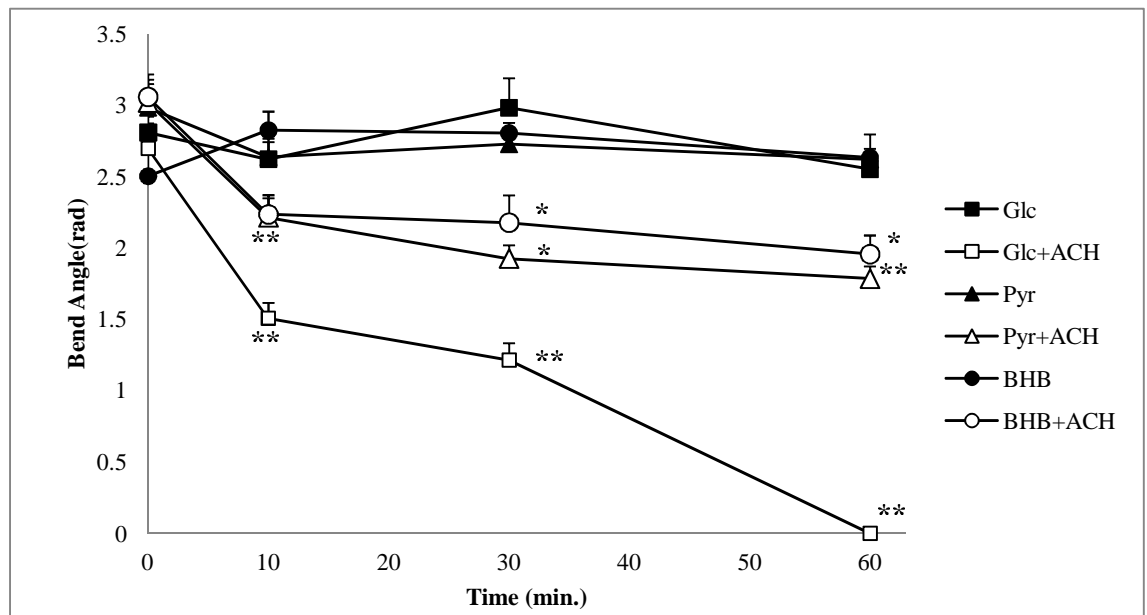
829

830   Figure 1: Effect of ACH on sperm flagellar motility in the presence of various substrates.

831

832

833   (C)   Shear angle
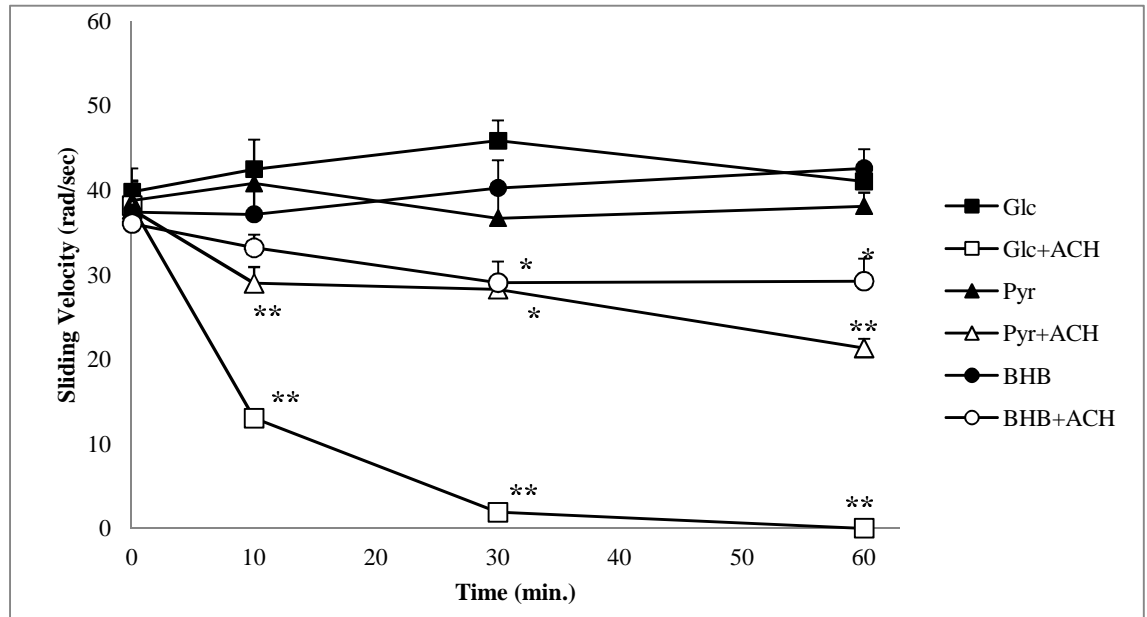
834

835   Figure 1: Effect of ACH on sperm flagellar motility in the presence of various substrates.

836

837

838   (A)
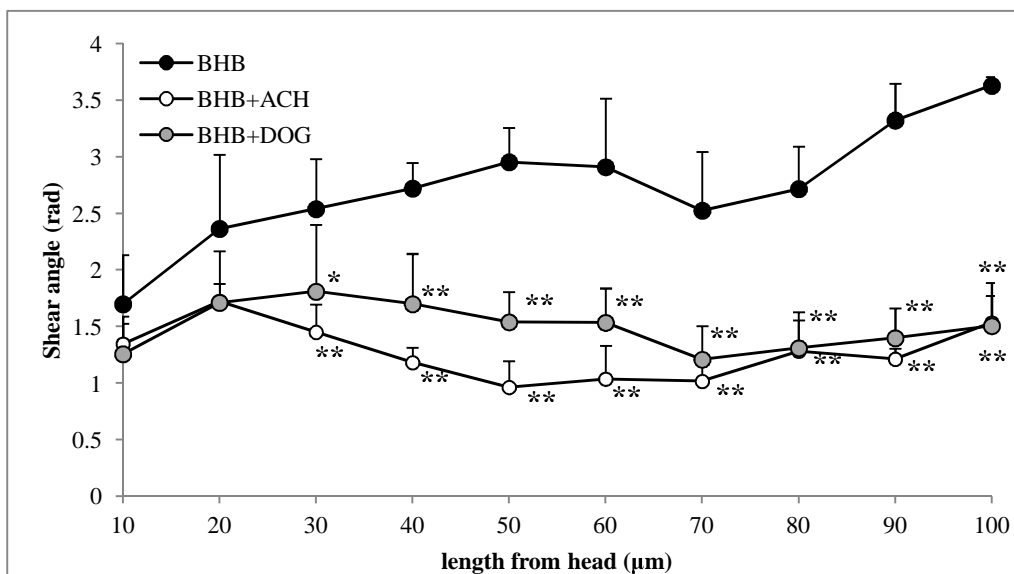
839

840   (B)
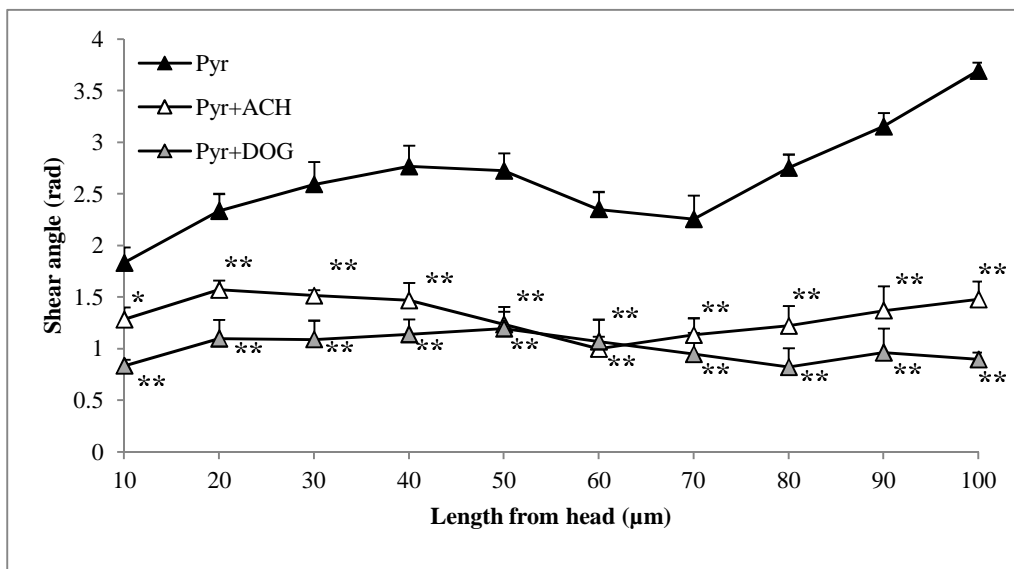
841

842   Figure 2: Changes of shear angle along the glycolysis-inhibited sperm flagella

843

844

845

846

(C)
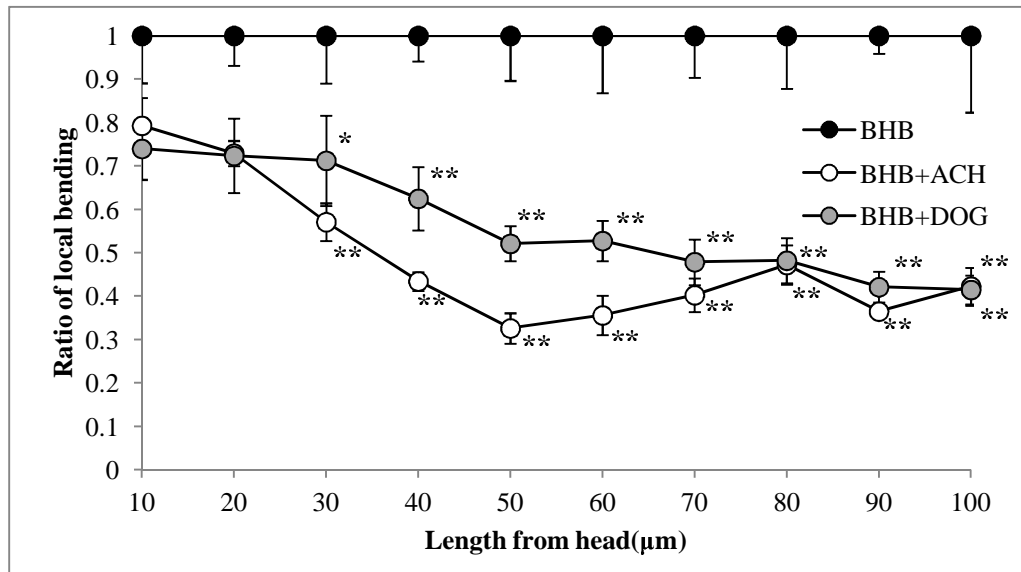
847

848

(D)
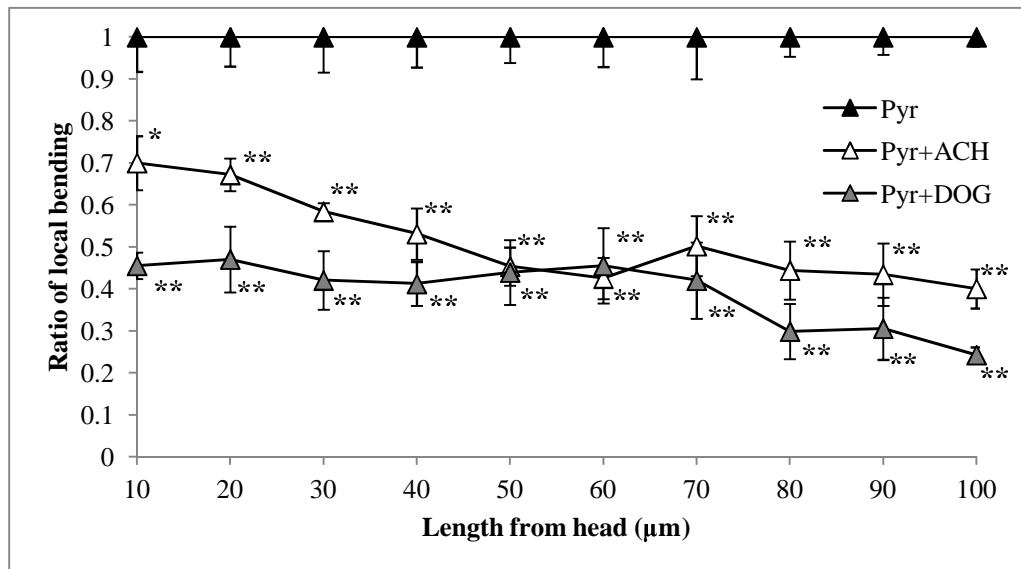
849

850 Figure 2: Changes in ratio of local bending along the glycolysis-inhibited sperm flagella

851

852
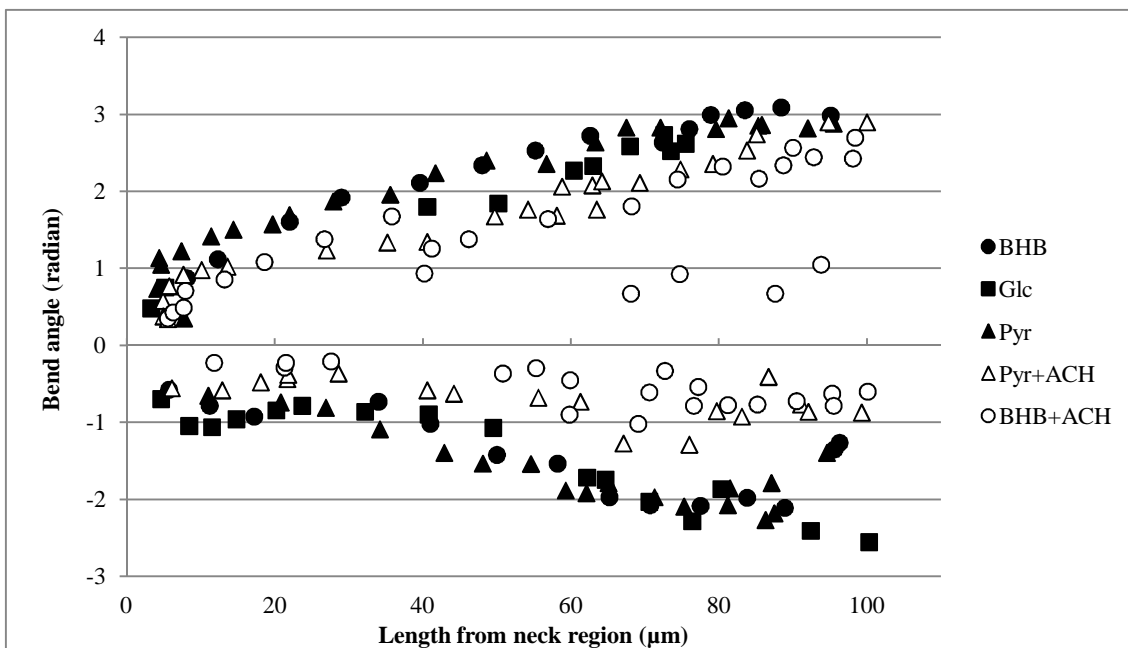
854   Figure 3: Scattergram of typical changes of local bend angle with the length of flagella

855

856

857
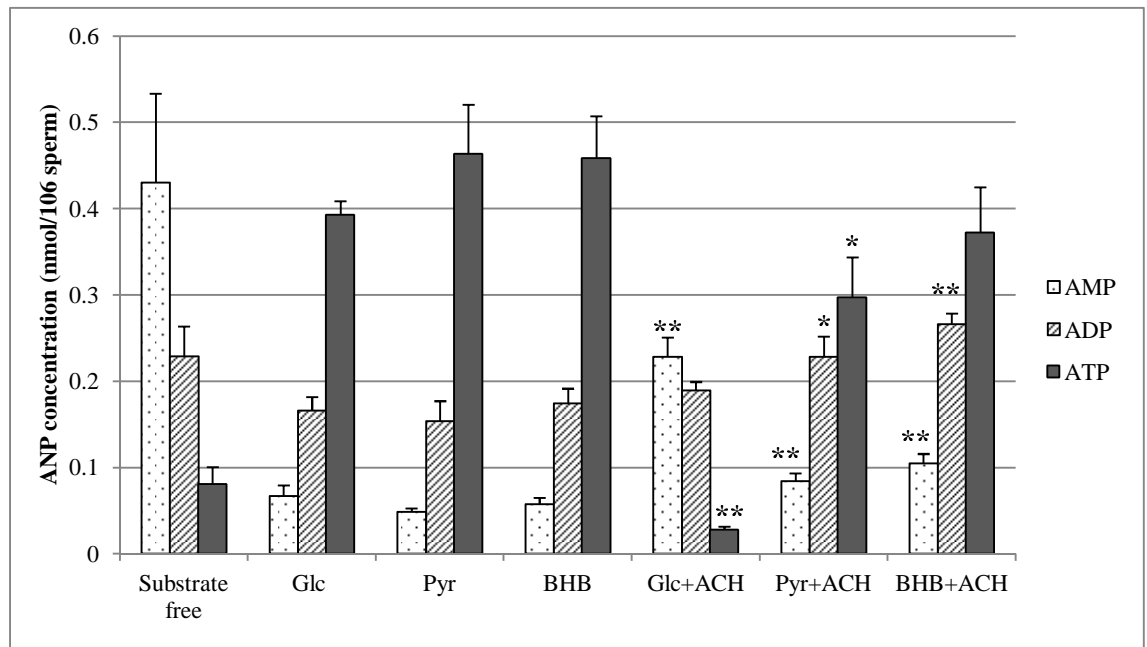
858

859 Figure 4: Effect of glycolytic inhibitor on the content of ANP in sperm.

860

861   (A)   ATP concentration profile along flagellum
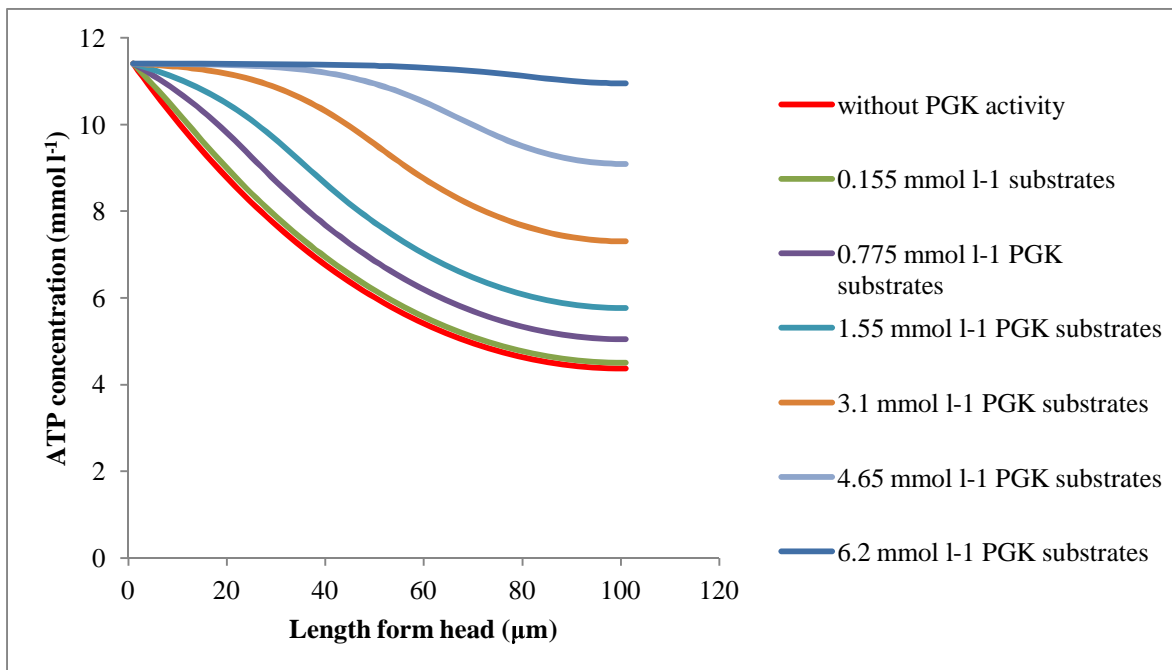
862

863

864   (B) ADP concentration profile along flagellum
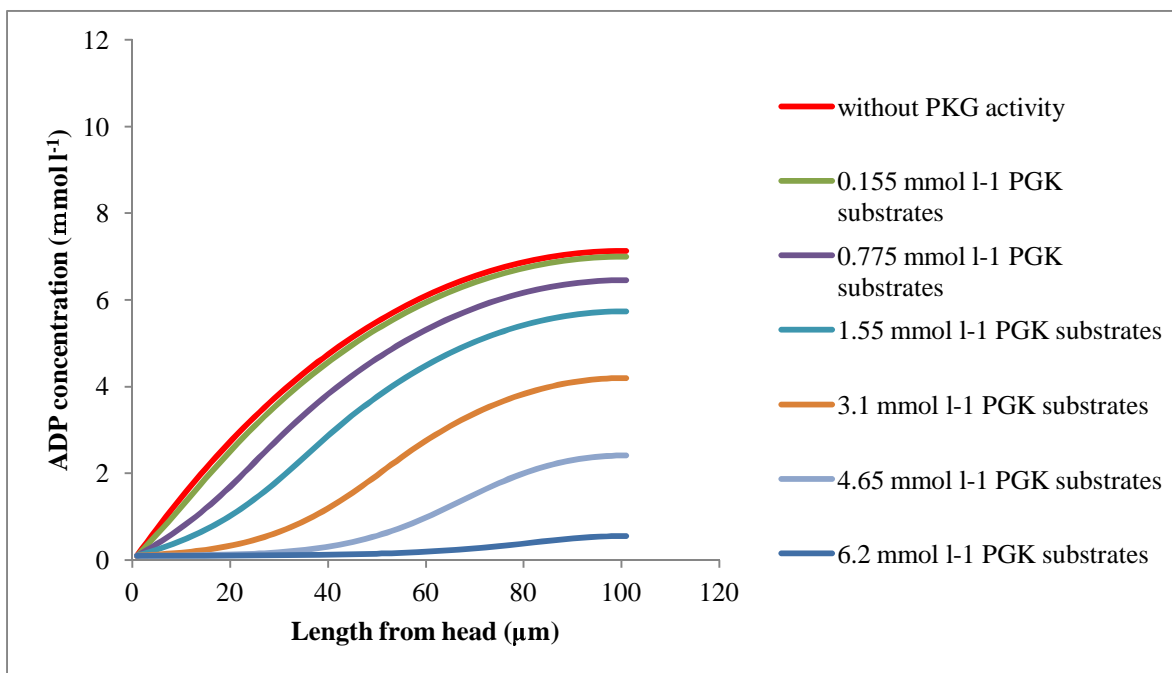
865

866

867   (C) ATPase activity profile along flagellum
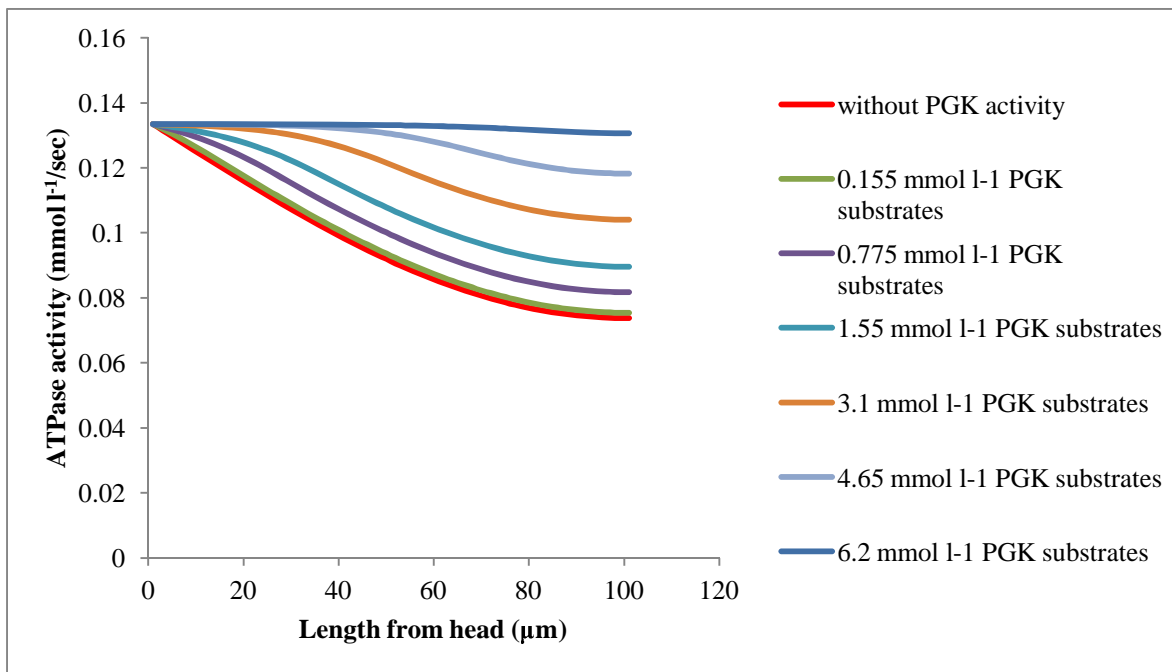
868

869

870   Figure 5: Simulation of high energy phosphoryls diffusion along the flagellum.

871

872
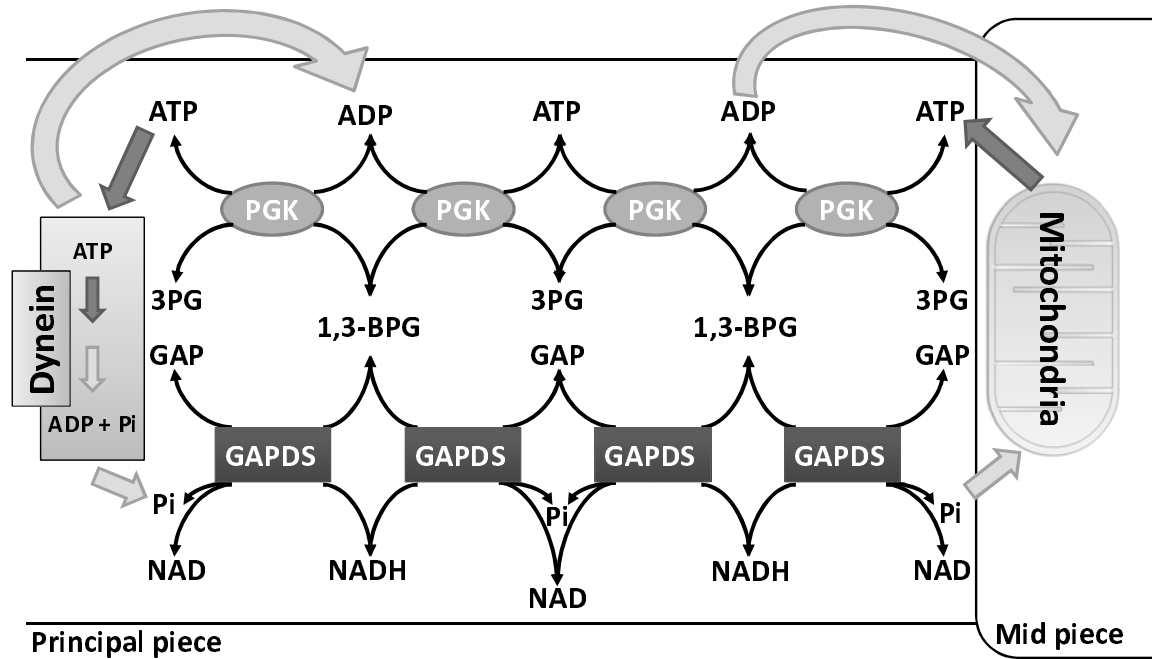
873

874   Figure 6: Schematic model of energy transfer system by glycolysis

875

876

877
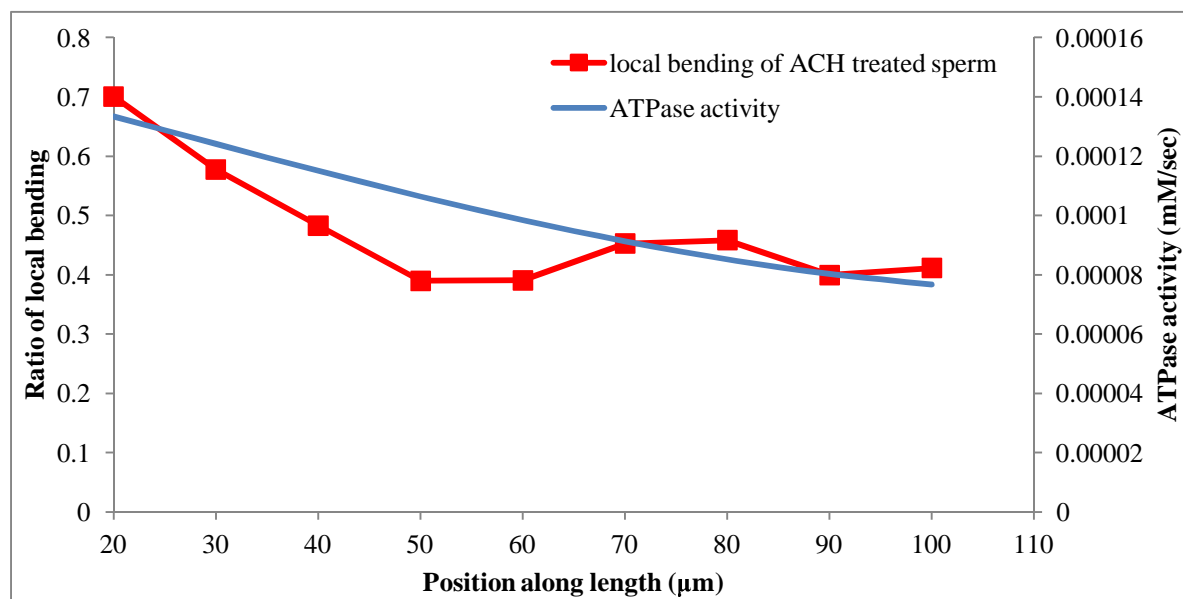
878

879   Figure 7: Superimposed schematic model of energy transfer system without glycolysis to the flagellar

880   local bending inhibited by ACH

881

882

883

884   (A) Bend angle
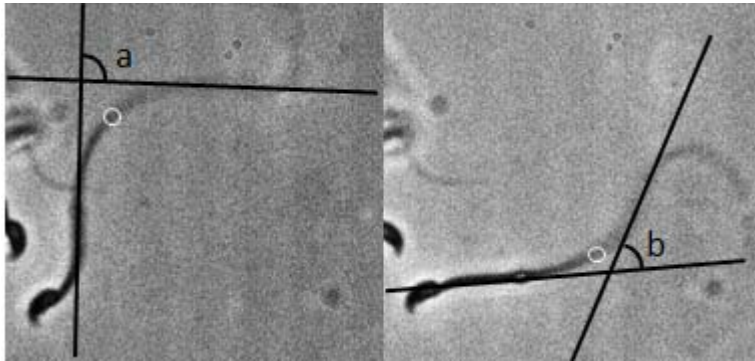
885

886   (B) Shear angle
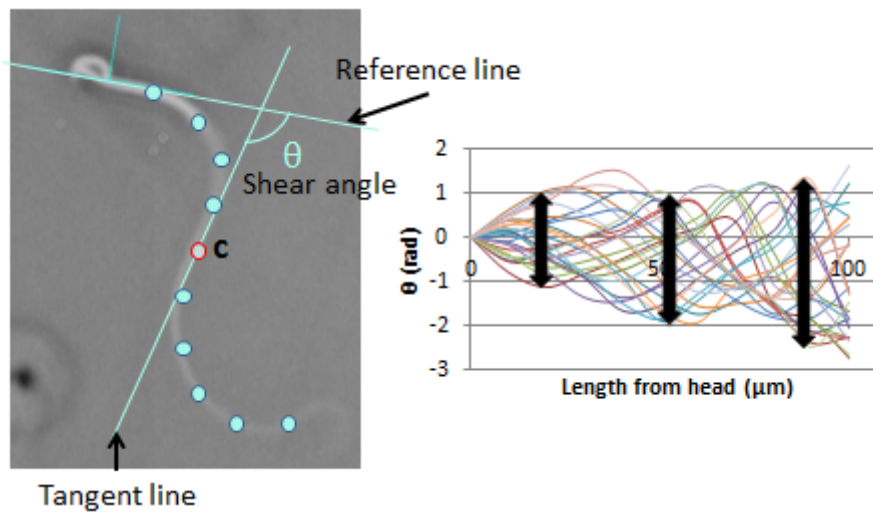
887

888   Figure 8: Methods for analysis of flagellar movement

889

1   **Tables**

2

3   Table 1. Difference of beat frequency, bend angle, sliding velocity and waveform of sperm flagella

4   depends on energy substrates.

	Glc n=16	Pyr n=9	BHB n=17
Beat Frequency (Hz)	16.3±0.70	14.6±0.72	16.9±1.13
Bend Angle (rad)	2.55±0.12	2.62±0.07	2.63±0.16
Sliding Velocity (rad/sec)	41.0±1.91	38.1±1.60	42.6±2.26
Motility (%)	55.8±4.60	58.8±2.43	56.3±3.92
Waveform			

5

6   Difference in beat frequency, bend angle, sliding velocity, percentage of motile sperm and typical

7   waveform by substrates are indicated. Data are represented as mean value ± s. e. m. No significant

8   difference in motility parameters was recognized. Concentration of substrates was 10 mmol l^{-1}.

9

10

11   Table 2. Parameters used for computations of Pi transport in flagella

Parameters	Value	Reference
Flagellar length	100 μm	See text
Diffusion coefficient for ANP	60 μm^{2}s^{-1}	Takao and Kamimura (2008)
Diffusion coefficient for 3PG and 1, 3 BPG	104 μm^{2}s^{-1}	Same as above
PGK substrates concentration (Total 3PG and 1, 3BPG)	0.155 mmol l^{-1}	Determined by metabolomic analysis
Total adenine nucleotide	11.6 mmol l^{-1}	Same as above
Q_{1F}	0.134 mmol l^{-1}/sec	Odet et al (2011)
Kl (K_m of ATPase from ATP, from ATP concentration for half-maximal beat frequency of demembranated flagella)	0.14 mmol l^{-1}	Ishijima, personal data
K_i (for inhibition of flagellar beat frequency by ADP)	0.28 mmol l^{-1}	Okuno and Brokaw (1979)
K_{mP} (PGK2 K_m value for 3PG)	1.55 mmol l^{-1}	Pegoraro and Lee (1978) Wolfgang and Theodor (1970)
K_{mT} (PGK2 K_m value for ATP)	0.32 mmol l^{-1}	Same as above
K_{mB} (PGK2 K_m value for 1, 3BPG)	0.0022 mmol l^{-1}	Same as above
K_{mD} (PGK2 K_m value for ADP)	0.16 mmol l^{-1}	Same as above
Q_{2R}/Q_{2F} (ratio of reverse to forward PGK2)	2.71	Same as above
K_A (myokinase K_m value for ATP)	0.3 mmol l^{-1}	Noda, (1973) [23]
K_N (myokinase K_m value for ADP)	0.3 mmol l^{-1}	Same as above
K_M (myokinase K_m value for AMP)	0.3 mmol l^{-1}	Same as above
Q_{3R}/Q_{3F} (ratio of reverse to forward adenylate kinase)	1.0	Same as above
Cytosolic volume	53.5 fL	Yeung et al., (2002) [40]

12

13

14

15 **Figures**

16   (A) Beat frequency
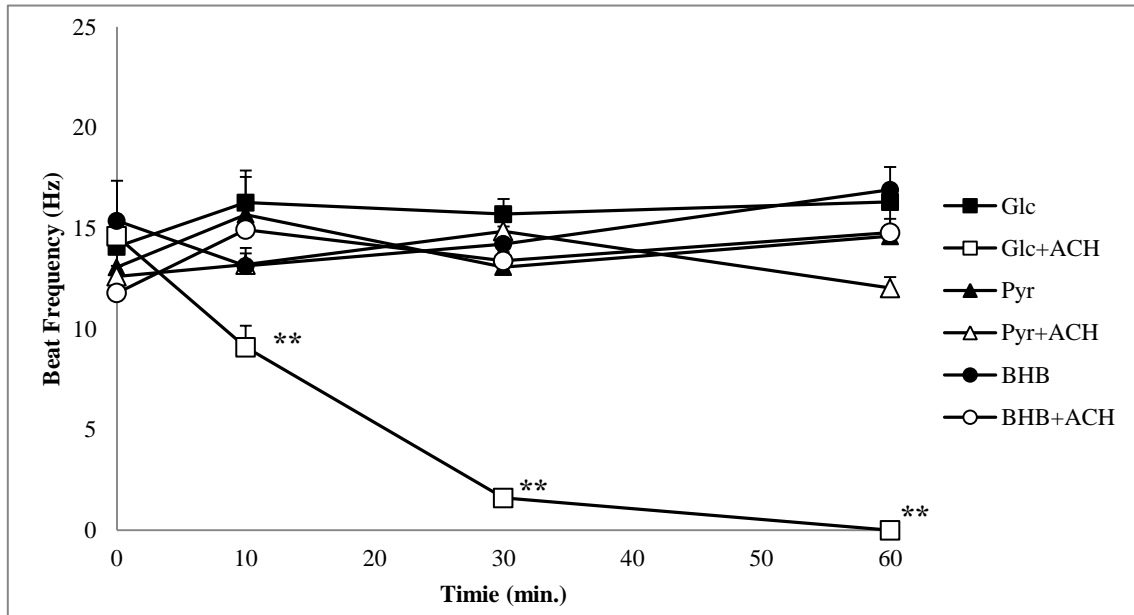
17

18   (B) Bend angle
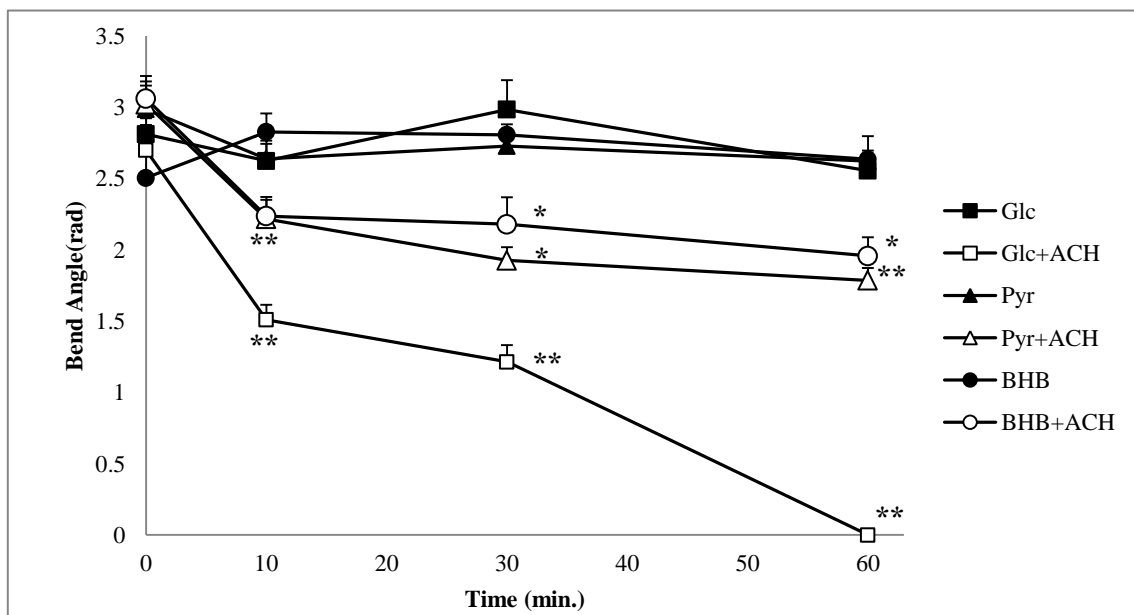
19

20   Figure 1: Effect of ACH on sperm flagellar motility in the presence of various substrates.

21

22

23   (C) Shear angle
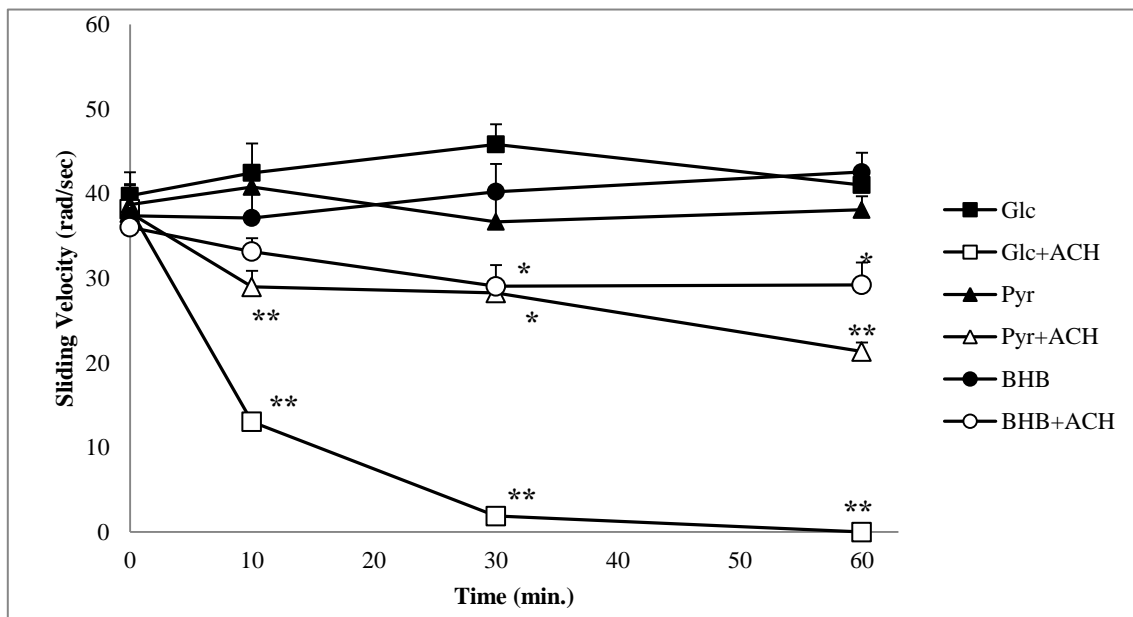
24

25   Figure 1: Effect of ACH on sperm flagellar motility in the presence of various substrates.
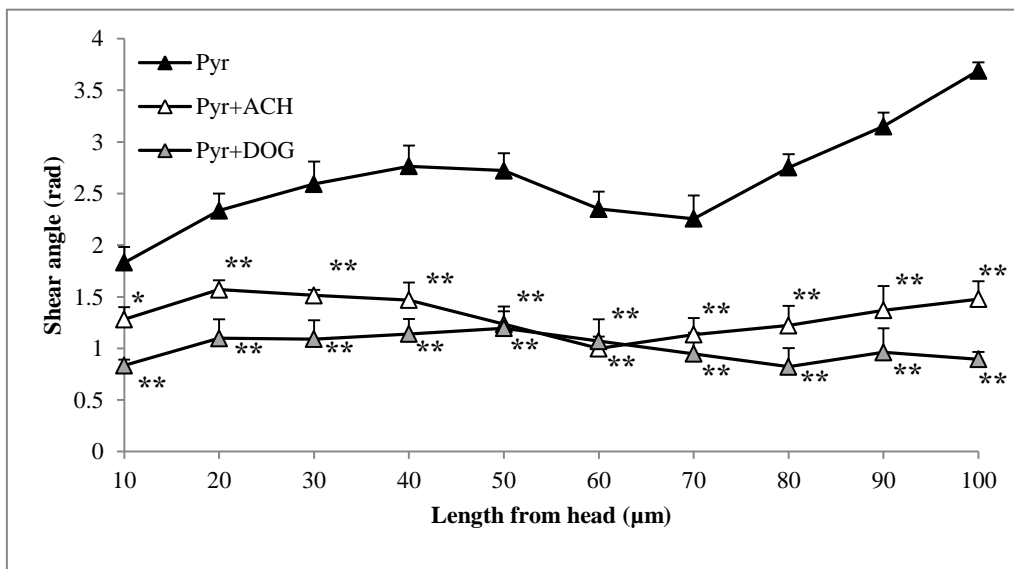
26

27

28   (A)
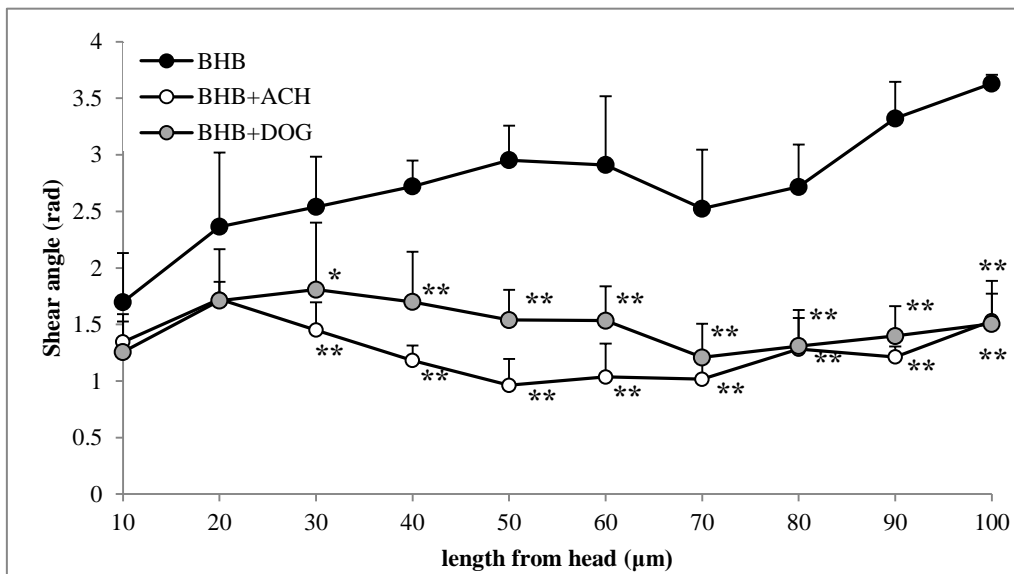
29

30   (B)

31

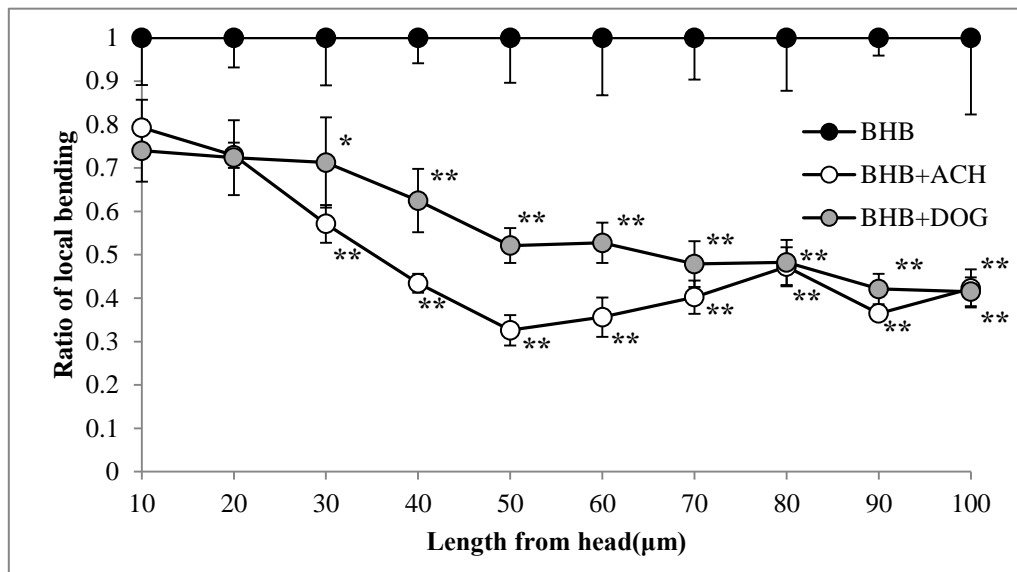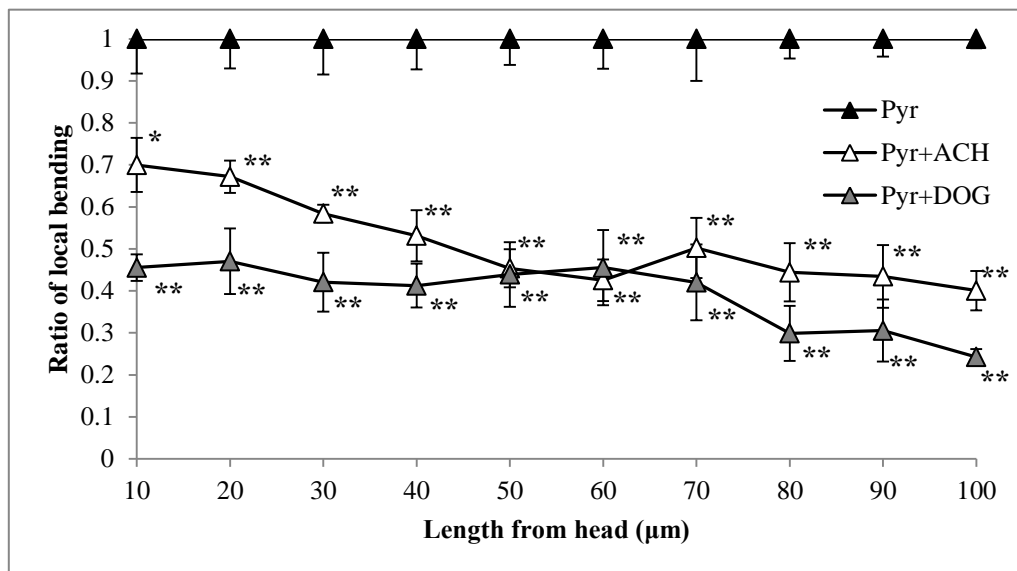32   Figure 2: Changes of shear angle along the glycolysis-inhibited sperm flagella
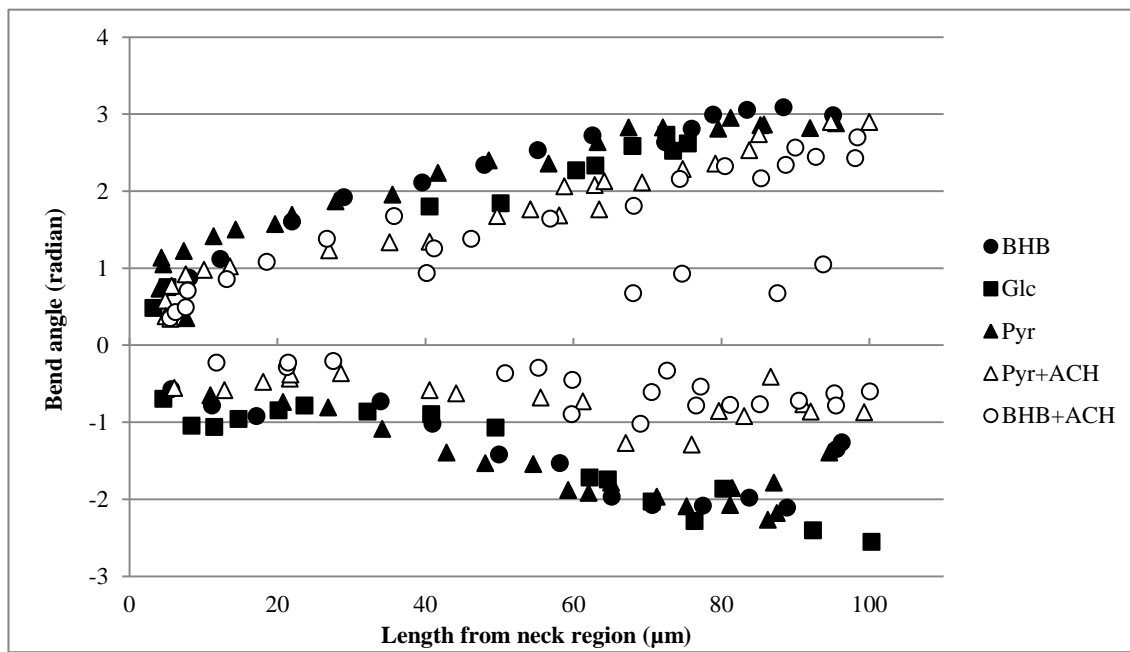
33

34

35

36   (C)

37

38   (D)

39

40   Figure 2: Changes in ratio of local bending along the glycolysis-inhibited sperm flagella

41

42

43

44 Figure 3: Scattergram of typical changes of local bend angle with the length of flagella

45

46

47
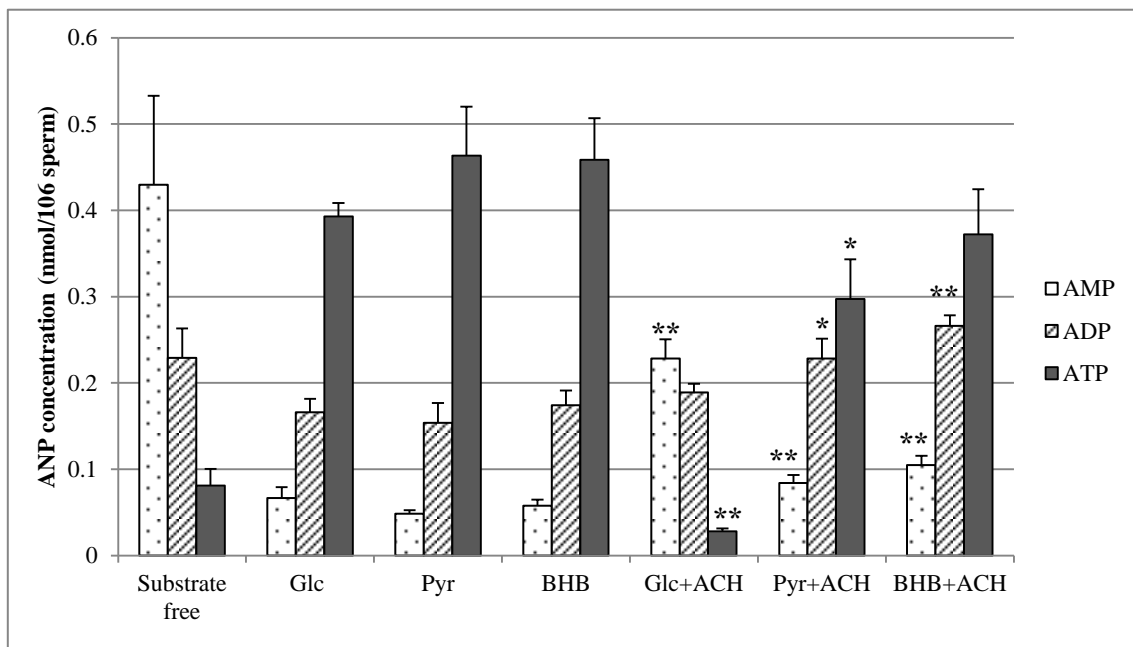
48

49   Figure 4: Effect of glycolytic inhibitor on the content of ANP in sperm.

50

51   (A) ATP concentration profile along flagellum
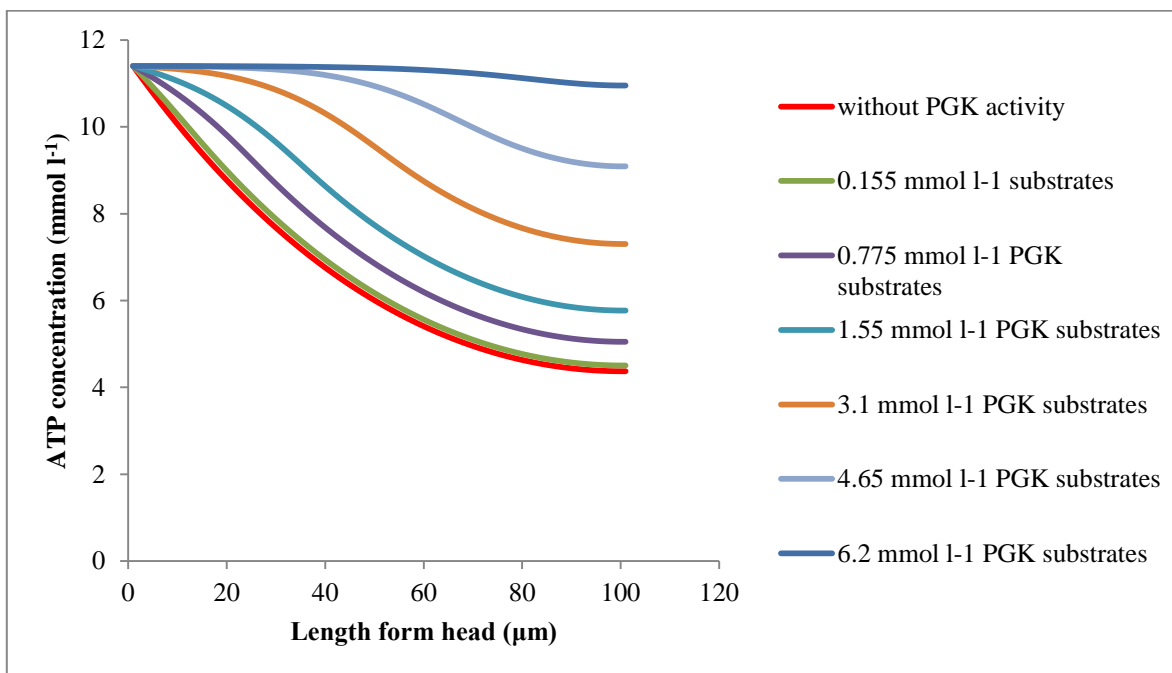
52

53

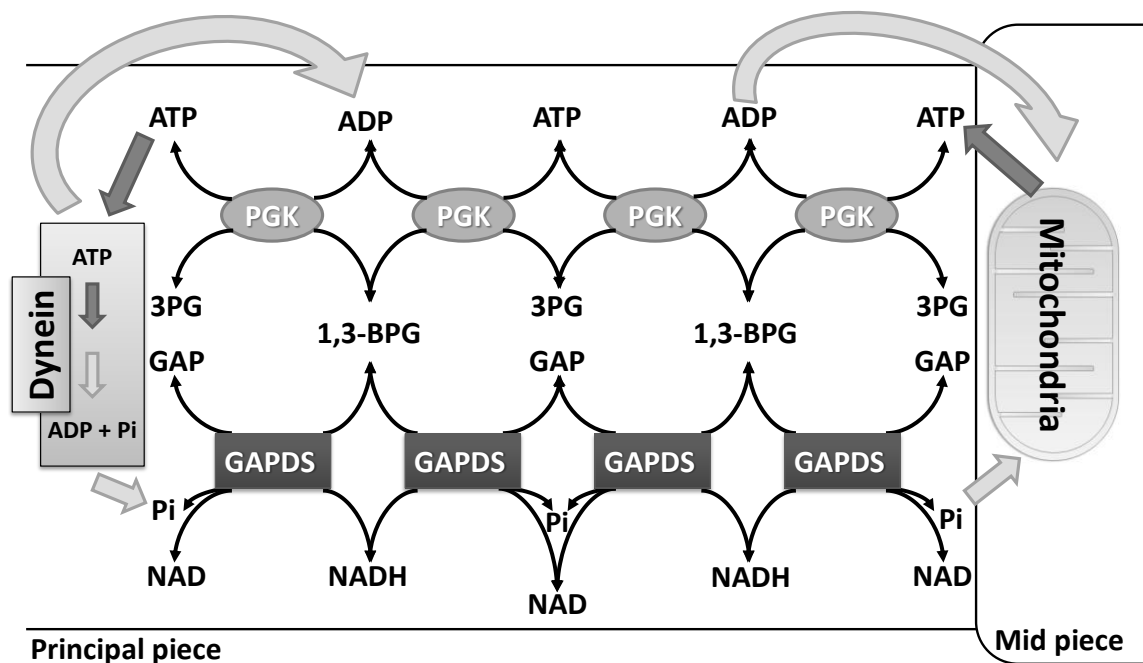54   (B) ADP concentration profile along flagellum
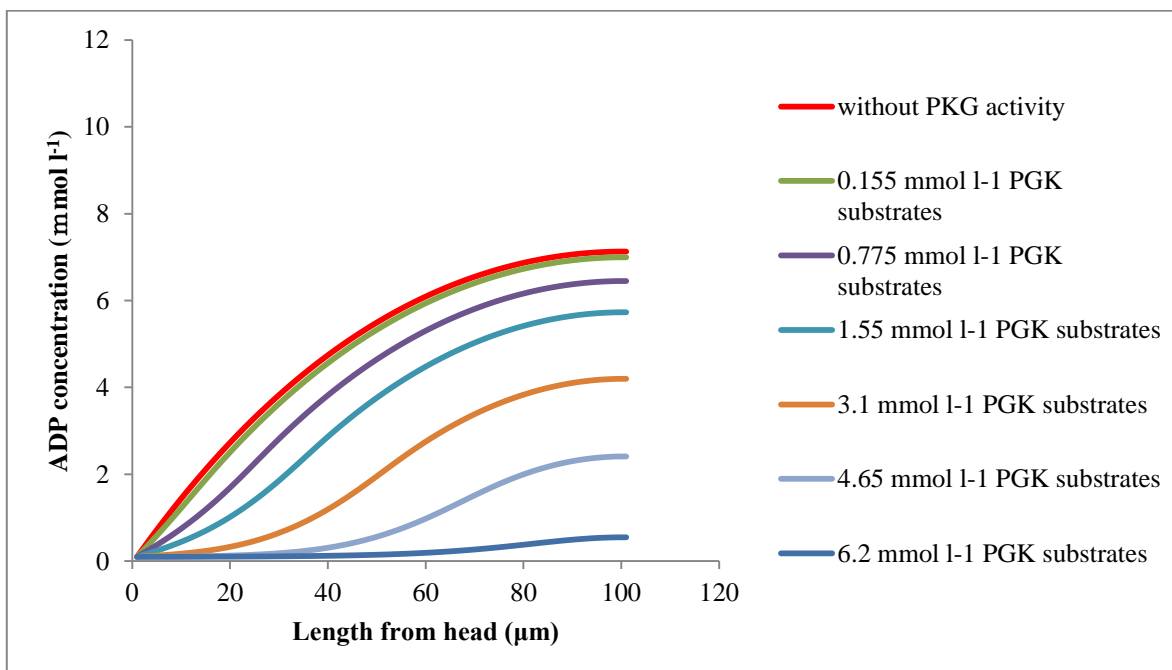
55

56

57   (C) ATPase activity profile along flagellum
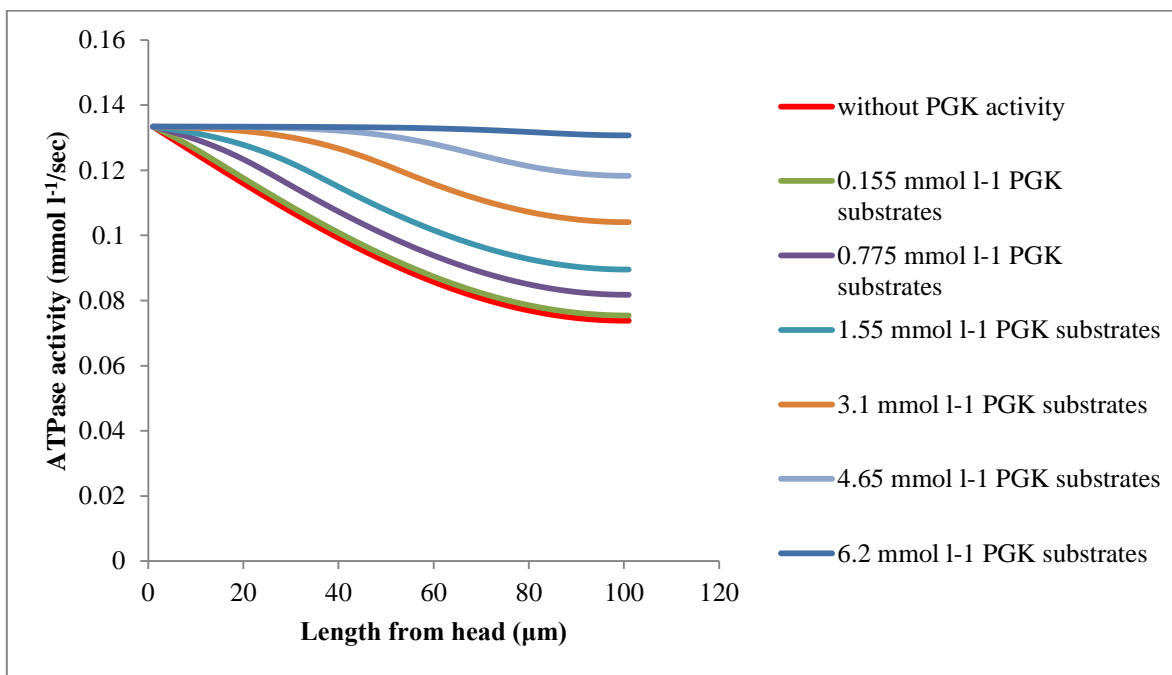
58

59

60   Figure 5: Simulation of high energy phosphoryls diffusion along the flagellum.
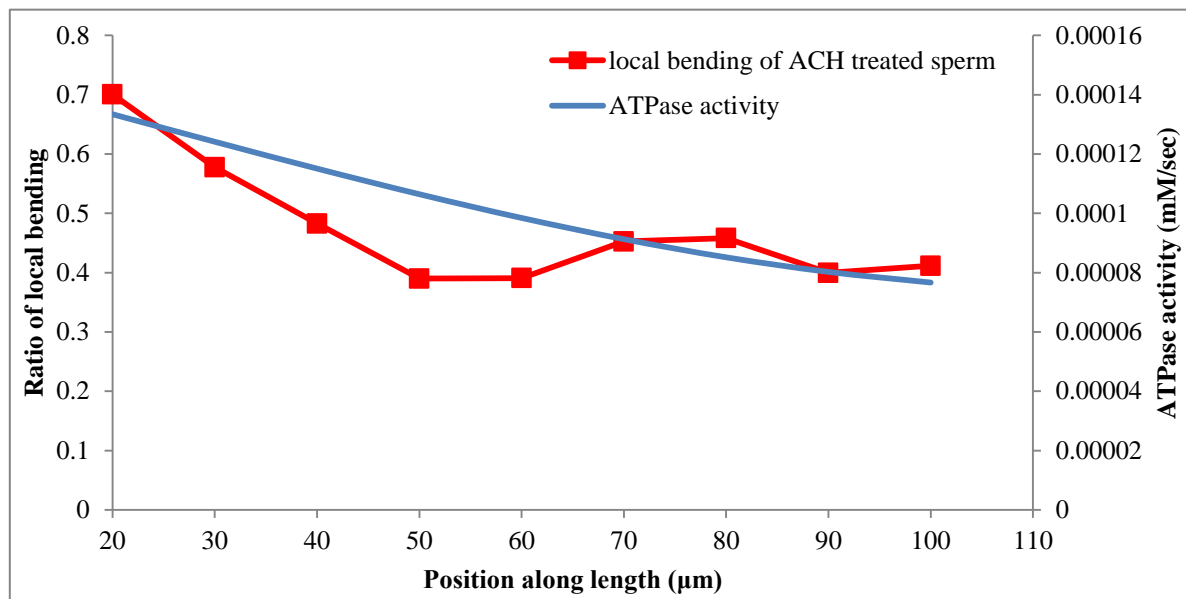
61

62

63

64   Figure 6: Schematic model of energy transfer system by glycolysis

65

66

67

68

69 Figure 7: Superimposed schematic model of energy transfer system without glycolysis to the flagellar
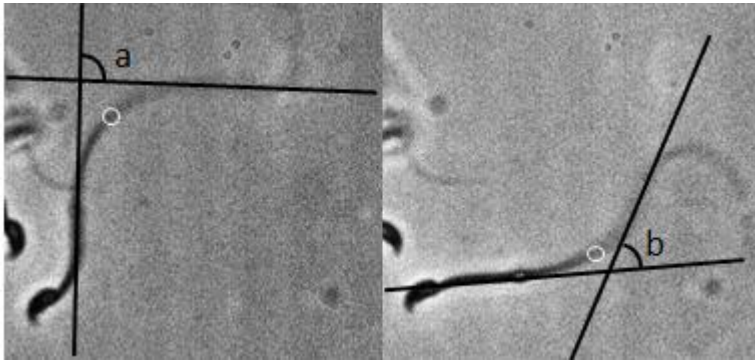
70 local bending inhibited by ACH
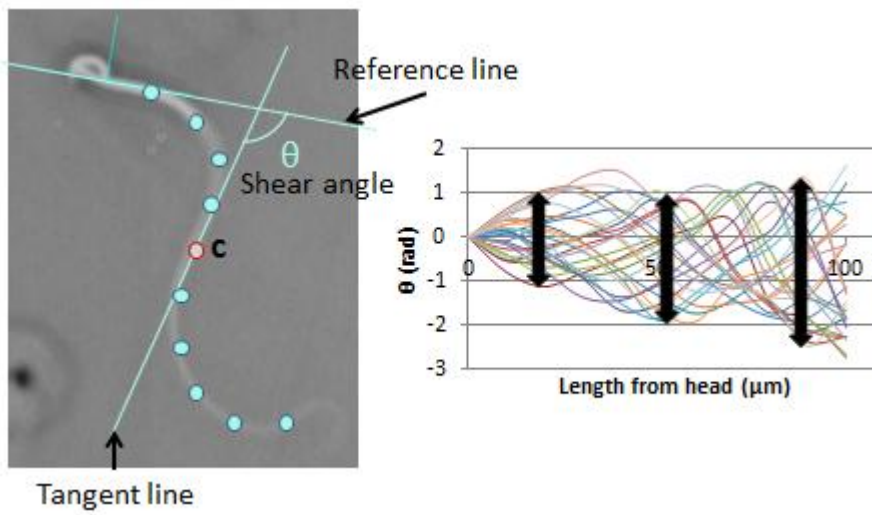
71

72

73

74   (A) Bend angle

75

76   (B) Shear angle

77

78   Figure 8: Methods for analysis of flagellar movement

79

80